

國立交通大學

顯示科技研究所

碩士論文

無轉態液晶反應單體修飾光學補償彎曲液晶盒之
研究



The study of Transition free Liquid Crystal Reactive
Monomer Modified OCB Cell

研究生：周蓮馨

指導教授：陳皇銘

中華民國九十七年六月

無轉態液晶反應單體修飾光學補償彎曲液晶盒之研究

The study of Transition free Liquid Crystal Reactive Monomer

Modified OCB Cell

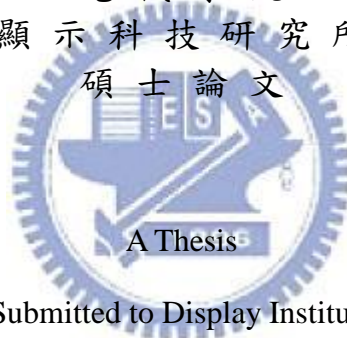
研究生：周蓮馨

Student : Liansing Chow

指導教授：陳皇銘

Advisor : Huang-Ming Philip Chen

國立交通大學
電機學院
顯示科技研究所
碩士論文



Submitted to Display Institute

College of Electrical Engineering

National Chiao Tung University

in Partial Fulfillment of the Requirements

for the Degree of

Master

In

Display Institute

June 2008

Hsinchu, Taiwan, Republic of China.

中華民國九十七年六月

無轉態液晶反應單體修飾光學補償彎曲液晶盒之研究

研究生：周蓮馨

指導教授：陳皇銘 博士

國立交通大學顯示科技所

摘要

在新興的 21 世紀，巨大的超級電腦已經被嬌小的筆記型電腦，或者是超薄型電腦取而代之，以往的大型 CRT 螢幕已經轉為超薄或是大型的液晶螢幕取代。液晶螢幕因為內部液晶的特殊電場反應，因而廣為社會大眾所使用，此外，液晶非常輕、薄、短、小，更有許許多多不同種類的液晶相繼問世，也形成大家爭相研究的對象之一。但液晶仍具有許多需要改良的地方，舉凡反應時間、以及動態影像品質，仍有很大的進步空間。而在這許多的液晶模式當中，光學補償彎曲液晶盒，也就是所謂的 Pi cell 或是 OCB cell，更為許多團體主要的研究對象。(optically compensated bend ,OCB 或稱 Pi-cell)。

光學補償彎曲液晶盒(OCB cell)，主要有三種狀態，首先在無電壓狀態下，其為 Splay 狀態，當加上一電壓大於臨界電壓則有 bend 狀態產生，這也是光學補償彎曲液晶盒主要操作範圍的起始點，同時也是亮態，當電壓加到很大時，則有液晶全部站直的狀態產生，同時也是主要的暗態，其特性為反應時間快，缺點為需提供一偏壓大於臨界電壓，方可啟動液晶，並達到可用的亮態區域。

本篇論文主要探討，如何使用新材料與原本的光學補償彎曲液晶盒配合，使得液晶得以不需加上一偏壓，在起始狀態即為亮態，並且維持原本的高對比度等優點。

The study of Transition free Liquid Crystal Reactive Monomer Modified OCB Cell

Student: Liansing Chow

Advisor: Dr. Huang-Ming Philip Chen

**Display Institute
National Chiao Tung University**

Abstract

In the newly 21st century, the giant super computer in the 20th century has been replaced by small and tiny notebooks or super thin computers. The CRT screen has been replaced by liquid crystal screen with a characteristic that very thin, very small, very light, and moreover, very short. The liquid crystal screen has a distinguishing feature that it responds to the electric field with different reactions. Accompany with different kind of liquid crystals be presented to the public, and some deficiencies with different kind of liquid crystal, like response time and the quality of the moving images, it becomes a new target to the researchers.

Among those different kinds of liquid crystals, optically compensated bend, also known as OCB cell or Pi cell, has a characteristic that its response time is fast and has high contrast ratio. OCB cell was operated at bend and vertical state, and also known has a big deficiency that it needs a voltage bigger than the critical voltage to have the splay state become the bend state, also called as transition.

In this thesis, we will discuss how to use a new material to operate with the original OCB cell and form the OCB cell in a condition without transition and still has the advantages of the original OCB cell.

誌謝

在這兩年的研究生活中，曾受到許多人的幫助，首要感謝的就是我的指導教授 陳皇銘老師以及師母，在我徬徨及需要意見的時候，適時給我客觀的建議及分析，幫助我做出適當的決定。在研究上，引導我深入液晶顯示領域，對於我的研究有莫大的幫助。

其次，感謝實驗室學長姐們—威慶、佳恬、昆展、鴻杰、耿睿、文孚、佑儒、俊民、廷綺、世民、宜揚的細心教導及建議，讓我慢慢進入狀況，知道做研究應該是怎麼回事，總是在生活上、研究中給我適當的幫助，以及同學們—怡帆、謹瑋、祥志，以及學妹—毓筠和其他的學弟妹，總是在你們忙的時候，抽空幫我分擔一些工作，幫助我的實驗可以順利完成。

最後，要向我的家人表達出我的感謝，謝謝你們一直默默的支持我，讓我順利的完成碩士的學業。



Table of contents

Abstract in Chinese	i
Abstract in English	ii
Acknowledgement	iii
Table of contents	iv
List of Tables	vi
List of Figures	vii
Chapter 1 INTRODUCTION AND BACKGROUND	1
1-1 INTRODUCTION OF LIQUID CRYSTALS	1
1-2 LIQUID CRYSTALS	1
1-2-1 Liquid crystal Phase	2
1-2-2 Phase 1-Nematic	3
1-2-3 Phase 2-Smectic	4
1-2-4 Phase 3-Cholesteric	4
1-2-5 Phase versus temperature	5
1-2-6 Liquid crystal optics	6
1-2-6-1 Light basic properties	6
1-2-6-2 Light wave's propagation in Nematic liquid crystal	8
1-3 SOME CHARACTERS AND STRUCTURE OF LCD	10
1-4 LCD OPERATION	10
1-5 OPTICAL COMPENSATED BEND (OCB) MODE OF LC	11
1-6 MOTIVATION AND OBJECTIVE	11
1-7 ORGANIZATION OF THIS THESIS	12
Chapter 2 OVERVIEW OF OCB CELL	13
2-1 THE CHARACTERISTICS OF OCB CELL	14
2-1-1 The structure of OCB cell	14
2-1-2 Fast response	16
2-1-3 Wide viewing angle	16
2-1-4 Nucleation and phase transition	18
2-1-5 Light leakage in dark state	20
2-2 SUMMARY	21

Chapter 3	MEASUREMENT SYSTEMS	22
3-1	ATOMIC FORCE MICROSCOPE	22
3-2	CELL GAP MEASUREMENT SYSTEM	25
3-3	LASER OPTICS SYSTEMS	29
3-4	POLARIZED OPTICAL MICROSCOPE	31
Chapter 4	EXPERIMENTS AND RESULTS	33
4-1	CELL FABRICATION PROCESS	34
4-2	CHARACTERISTICS OF REACTIVE NEMATIC LC MONOMERS	38
4-3	NOVEL OCB-CELL MODEL	39
4-4	MEASUREMENT OF ELECTRO-OPTICAL PROPERTIES AND RESULTS	41
4-4-1	Phase transition free OCB cell	41
4-4-2	Retardations	44
4-4-3	RMM surface tilt angle	45
4-4-4	Contrast ratio	46
4-5	SUMMARIES	49
Chapter 5	CONCLUSIONS	50
5-1	SUMMARY	50
5-2	FUTURE WORKS	51
References		52



List of Tables

Table 4-A	Parameters of spin coating polyimide.....	35
Table 4-B	Rubbing Conditions for Polyimide glasses.....	35
Table 4-C	Parameters for RMM-19B.....	36
Table 4-D	The parameters of liquid crystal ZCE-5096XX.....	37
Table 4-E	RMM thickness with spin coating speed's relation.....	40
Table 4-F	4wt% RMM-OCB cells and conventional OCB cell-1.....	42
Table 4-G	4wt% RMM-OCB cells and conventional OCB cell-2.....	42
Table 4-H	The transmittance of RMM2-OCB cell when in different include θ	44
Table 4-I	FLC-RMM cell, Δn of RM when $\theta=0$	46
Table 4-J	Δn of RMM-OCB cell and pretilt angle.....	46
Table 4-K(a)	Contrast ratio of RMM-OCB cells and conventional OCB cell-1.....	47
Table 4-K(b)	Contrast ratio of RMM-OCB cells and conventional OCB cell-2.....	47



List of Figures

Fig 1-A	Types of rod-liked liquid crystals, (a) Nematic, (b) Smectic (A type), and (c) cholesteric liquid crystal.....	2
Fig 1-B	The main axis of Nematic liquid crystal.....	3
Fig 1-C	Smectic has layer structure because of the two orientations.....	4
Fig 1-D	Cholesteric liquid crystals' helical structure, it can reflect the incident light....	5
Fig 2-A	OCB cell's structure and five configurations.....	14
Fig 2-B	Schematic figure of the dynamics in the pi-cell. The flow induces the torque to accelerate to relax.....	15
Fig 2-C	(a) Splay state, (b) V_{off} (V_{cr}), bend mode, and OCB cell is in the bright state. (c) V_{on} , homeotropic state, and OCB cell is in the dark state.....	16
Fig 2-D	Experimental results of the viewing-angle-dependent transmittance for TN cell and OCB cell.....	17
Fig 2-E	Cross-section view of OCB cell, it has symmetric viewing angle.....	17
Fig 2-F	Mechanism of bend transition.....	18
Fig 2-G	The pretilt angle versus energy distribution of splay state and bend state.	19
Fig 2-H	Gibbs's free energy of bend and splay states as a function of applying voltage.....	19
Fig 2-I	The LC molecules alignment of (a) VA mode, and (b) dark state of OCB cell.....	21
Fig 3-A	(a) Block Diagram of Atomic Force Microscope (b) Concept of AFM and the optical lever.....	23
Fig 3-B	UV/Vis spectrometer LAMBDA 950 from Perkin Elmer.....	26
Fig 3-C	Two surfaces possess reflective index R1 and R2, light would pass through surface 1 and 2 and causing a light interference.....	27
Fig 3-D	The spectrum result for the sample as an example.....	28
Fig 3-E	The scheme of laser optic system.....	29
Fig 3-F	(a) the installation of retardation measurement(b) LC cell position.....	30
Fig 3-G	The picture of POM.....	31
Fig 4-A	Fabrication process of OCB cells.....	34
Fig 4-B	The two different types: (a) only the bottom substrate uses RMM layer glasses. (b) Both substrate use RMM layer on it.....	37
Fig 4-C	The scheme of RMM-OCB cell under (a) 0V, (b) 6V.....	39
Fig 4-D	RMM-19B microscopic structure observed by AFM. RMM-19B forms a thin film about 100~200 nm with 3 nm roughness.....	40
Fig 4-E	The pictures of RMM-19B when in (a) dark state and (b) bright state.....	40

Fig 4-F	The relation between the RMM layer's thickness and the cell's Critical voltage corresponds to different spacers.....	41
Fig 4-G	The include angle $\theta=45^\circ$ between RMM-OCB cell's rubbing direction and polarizer's direction.....	42
Fig 4-H	Different thickness of RMM layers with (a) cell gap around 5 μ m, and (b) cell gap around 3 μ m, and (c) RMM layer on both substrates.....	43
Fig 4-I	(a) is conventional OCB cell's retardation (b) on the right is retardations of the RMM-OCB cells under applied voltage from 0V to 6V with different viewing angle.....	44
Fig 4-J	(a) RMM-OCB cell under 7V (b) conventional OCB cell under 7V.....	48
Fig 4-K	(a) RMM-OCB cell under 0V (b) conventional OCB cell under 2V.....	48
Fig 4-L	(a) Contrast state of RMM-OCB cell (b) contrast state of conventional OCB cell.....	48



CHAPTER 1

INTRODUCTION AND BACKGROUND

1-1 INTRODUCTION OF LIQUID CRYSTALS

Liquid crystalline phase is first discovered by Dr. F. Reinitzer [1] in 1888 and the well known term “liquid crystal” is introduced by Lehmann [2] in 1890. Liquid crystals are substances that exhibit a phase of matter that has properties between those of an isotropic liquid, and those of a solid crystal.

In these years, Internet and digital information market grow up fast beyond imagination. Because LC display has many advantages, such as thin, light weight, low power consumption, no radiation pollution, and the most important, compatible with semi-conductor technology, the application of LC display has grown up fast, too. The technology includes material, equipment, manufacture, and product character’s development. Until today, the LC displays are still growing up with amazing speed, and become the lead of planar display market.

1-2 LIQUID CRYSTALS

In 1888, Austrian botanical physiologist Friedrich Reinitzer found that cholesteryl benzoate does not melt like other compounds, but had two melting points. At 145.5°C it melted into a cloudy liquid, and at 178.5°C it melted again and the cloudy liquid became clear. Next year, Otto Lehmann, a physicist from Karlsruhe, Germany, found out the birefringence

character of liquid crystal, the optical anisotropic. In 1890, these two people called the new phase of matter liquid crystal as fourth state of matter or meso-phases.

1-2-1 LIQUID CRYSTAL PHASE

Liquid crystal phase is a state between solid state and liquid state, also called the forth state. As a result, it has both the solid character and liquid characters. The structure is similar to crystal's arrangement, and the liquid character can help the molecule change the position and point direction.

The structures of LC molecules are asymmetric, can be classified into two major shapes, rod-liked and disk-liked. Rod-liked molecules tend to orient themselves around the rubbing direction of the substrate, and align parallel to each other to a preferred direction which is so called self-assembly. To be more accurate, Rod-liked liquid crystal material can be divided into three major types of liquid crystals—Nematic, Smectic, and Cholesteric.(Fig.1-A)

Liquid crystals have another important character, uni-axial anisotropy. This character can let Liquid crystals have different refractive index, magnetic susceptibility, dielectric constant in different orientation.

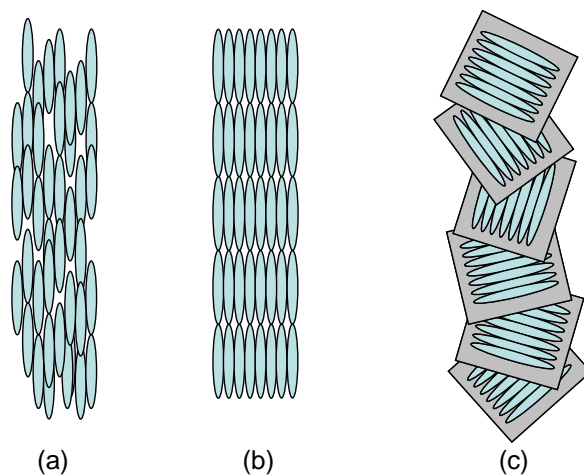


Fig. 1-A: Types of rod-liked liquid crystals, (a) Nematic, (b) Smectic (A type), and (c) cholesteric liquid crystal.

1-2-2 PHASE 1- NEMATIC

Nematic is a kind of liquid crystal that most like the liquid. Nematic has small viscosity and fast response time. It's the earliest liquid crystals that been used in LC TV, monitor, and all types of display elements [3, 4, 5]. It has the worst alignment compare to other liquid crystal. Nematic has a main axis that all molecules would roughly point toward the direction, like the “n” direction in (Fig. 1-B). We can define the direction “n” as a vector.

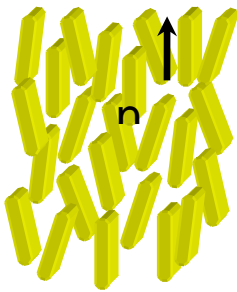
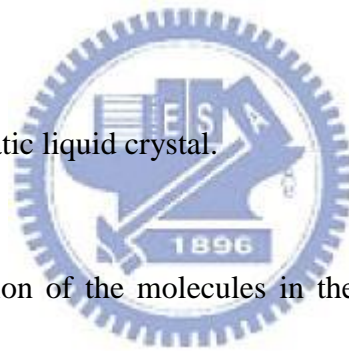


Fig. 1-B: The main axis of Nematic liquid crystal.



We also present the direction of the molecules in the liquid crystal as a function like Equation (1-1).

$$S = \frac{1}{2} \langle 3\cos^2\theta - 1 \rangle \quad \text{Equation (1-1)}$$

“S” is the order parameter, θ is the angle between molecule’s long axis and **n**. “S” would be “0” when in isotropic state, and “1” when in a solid state. As a result, when molecules aligned perfectly parallel, $\theta=0$, and S will be “1”, the light will pass and the liquid crystal would be transparent. When molecules aligned randomly, $\theta=\text{random}$, S will be “0”, the light can’t pass. Generally, liquid crystal molecules have $0.5 < S < 0.7$.

1-2-3 PHASE 2- SMECTIC

On the contrary, Smectic is a kind of liquid crystal that most like the solid. Smectic has high viscosity and slow response time, so their main application is optical data storage materials, they are rarely been used in displays.

Smectic has two orientation of alignment, so they can align like layers (Fig. 1-C). It has different aligned directions in different layers, but the molecules in the same layer would tend to have the same aligned direction. Smectic can be classified into A to L 12 different kinds and named in the order by the time they were found. For example, Smectic A phase, Smectic C phase. In Smectic A phase, the molecules align perpendicular to the layer planes, and in Smectic C phase the alignment of the molecules is at some arbitrary angle to the normal.

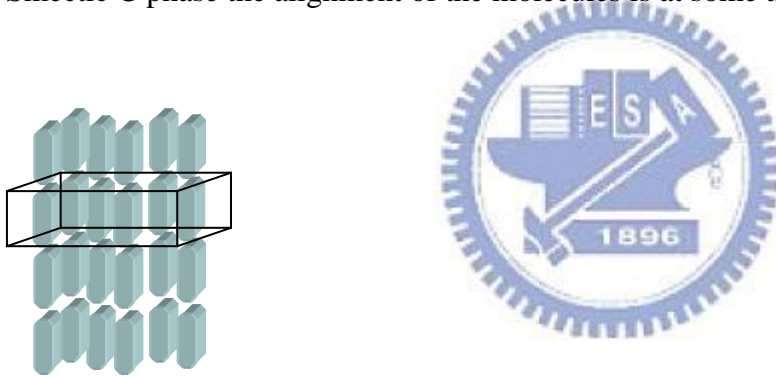


Fig. 1-C: Smectic has layer structure because of the two orientations.

1-2-4 PHASE 3- CHOLESTERIC

Cholesteric liquid crystal, also called “Chiral Nematic liquid crystal”, is stacked by many layers of Nematic liquid crystals, and aligned in helical planes that parallel with each other. Each surface has different long axis, the adjacent long axes have an included angle.

When the two adjacent long axes have the same orientation, the distance between the two planes calls a pitch (Fig. 1-D). The pitch will change with different temperature, pressure, electric field, or magnetic field. Besides, Cholesteric has optical rotation, it can reflect the

incident light with $2\pi n$ (n is average refractive index). Therefore, when the temperature changed, it will have a selective reflection because of different wavelengths and causes a color variation. As a result, it can be used as a temperature sensor. Besides, the alignment of molecules are easily been affected by the electric field, it also can be used as reflective displays, and electronic paper [6].

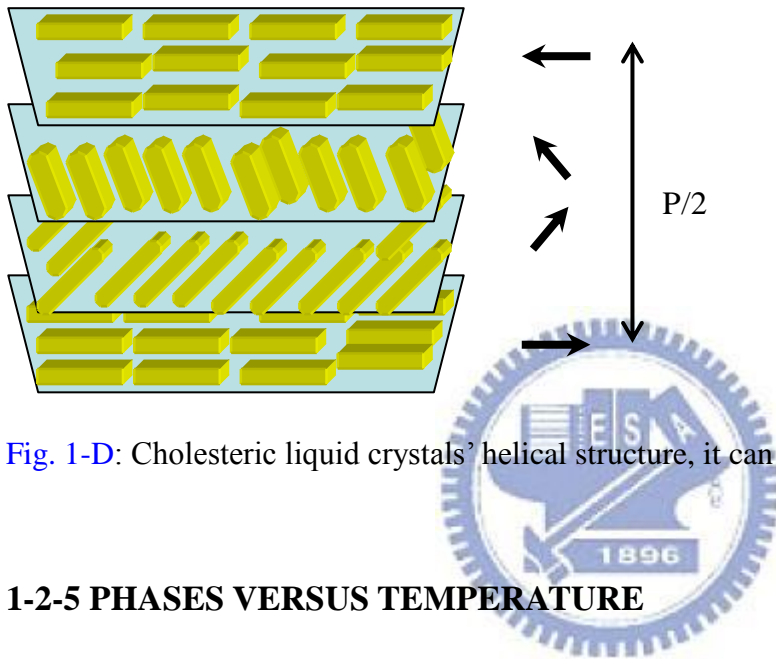


Fig. 1-D: Cholesteric liquid crystals' helical structure, it can reflect the incident light.

1-2-5 PHASES VERSUS TEMPERATURE

The different alignment of liquid crystals accompany with the change of temperature can be expressed as follows:

Solid → Smectic → Nematic → Isotropic

Crystal → Liquid Crystal → Liquid

Low temperature → High temperature

The alignment of molecules will become isotropic and liquid when the temperature is higher than the clearing point, also called T_{N-1} . At this point, liquid crystal will become clear and transparent.

1-2-6 LIQUID CRYSTAL OPTICS

When light passes through liquid crystals, it can have some effect like refraction, interference, diffraction, and polarization. Light is a kind of electromagnetic wave and has also can be divided into different kinds and colors by different wavelength. As a result, we will discuss only the monochromatic plane light wave in the following.

1-2-6-1 Light basic properties

From Maxwell equations, we can derive wave equations:

$$\vec{\nabla} \times (\vec{\nabla} \times \vec{E}) + \frac{1}{c^2} \frac{\partial^2 \vec{E}}{\partial t^2} = -\mu_0 \frac{\partial^2 \vec{P}}{\partial t^2} - \mu_0 \frac{\partial \vec{J}}{\partial t} \quad \text{Equation (1-2)}$$

For a generalized three dimensional monochromatic plane light wave, it propagate in a uniform dielectric substance, then $\vec{P} = \epsilon_0 \chi \vec{E}$, and $\vec{J} = 0$.

$$\vec{\nabla} \times (\vec{\nabla} \times \vec{E}) + \frac{n^2}{c^2} \frac{\partial^2 \vec{E}}{\partial t^2} = 0 \quad \text{Equation (1-3)}$$

The refraction index could be: $v = \frac{c}{n} \Rightarrow n \equiv \sqrt{\mu\epsilon}$

From Equation (1-3), we can get wave function as:

$$\vec{E}(\vec{r}, t) = \vec{A} \cos[\omega t - \vec{k} \cdot \vec{r} + \delta] \quad \text{Equation (1-4)}$$

Because light is a transverse wave, the polarization direction is the direction of the electric field. We define the travel direction as z direction, so the electric field of monochromatic plane light wave will vibrate in x-y plane.

Then we can rewrite Equation (1-4) as two vectors perpendicular with each other.

$$E_x = A_x \cos(\omega t - kz + \delta_x)$$

$$E_y = A_y \cos(\omega t - kz + \delta_y) \quad \text{Equation (1-5)}$$

$A_x, A_y, \delta_x, \delta_y$, represents the amplitude of vibration and the phase individually. To

describe the polarization of light wave simply, take $z=0$ to see the change of the vibration verses time on the x-y plane, then Equation (1-5):

$$E_x = A_x \cos(\omega t + \delta_x)$$

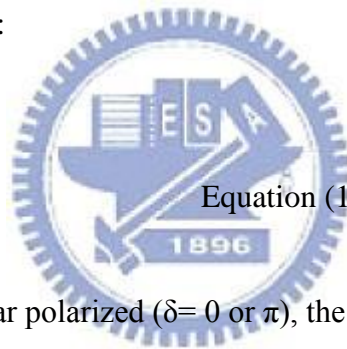
$$E_y = A_y \cos(\omega t + \delta_y) \quad \text{Equation (1-6)}$$

We can define the phase as: $\delta = \delta_y - \delta_x$. If $\delta = 0$ or π , then

$$E_y = \frac{A_y}{A_x} E_x, \text{ or } E_y = -\frac{A_y}{A_x} E_x \quad \text{Equation (1-7)}$$

From Equation (1-7), when the electric field vibrates in $\frac{E_y}{E_x}$ direction, we call it as linear polarization state. We use a new math calculate way to describe the polarization state of light--- Normalized Jones Vector:

$$J = \frac{1}{\sqrt{A_x^2 + A_y^2}} \begin{pmatrix} A_x e^{i\delta_x} \\ A_y e^{i\delta_y} \end{pmatrix} \quad \text{Equation (1-8)}$$



When the light wave is linear polarized ($\delta = 0$ or π), the x axis has an included angle of Ψ , then:

$$J_\psi = \begin{pmatrix} \cos \psi \\ \sin \psi \end{pmatrix} \quad \text{Equation (1-9)}$$

And

$$J_\psi * J_{\psi + \frac{\pi}{2}} = 0 \quad \text{Equation (1-10)}$$

So the two factors are orthogonal with each other. When $\Psi=0$:

$$J_x = \begin{pmatrix} 1 \\ 0 \end{pmatrix}, \text{ and } J_y = \begin{pmatrix} 0 \\ 1 \end{pmatrix} \quad \text{Equation (1-11)}$$

The index of J means the x polarized direction and y polarized direction.

1-2-6-2 Light wave's propagation in Nematic liquid crystal

When we consider Nematic liquid crystal cells as uni-axial and anisotropic medium, we can have the light effects as follows:

In uni-axial medium, we have three refraction indexes as n_x , n_y , n_z .

We have: (1) $n_x = n_y = n_o$, calls ordinary index.

(2) $n_z = n_e$, calls extraordinary index.

When $n_e > n_o$, the medium were named as positive uni-axial medium. When $n_e < n_o$, the medium would be negative uni-axial medium.

We can get two modes from light propagate in uni-axial medium, ordinary wave and extraordinary wave.

We can present the two refractive indexes as:

O wave : $n = n_o$ Equation (1-12)

E wave : $\frac{1}{n_e(\theta)^2} = \frac{\cos^2\theta}{n_o^2} + \frac{\sin^2\theta}{n_e^2}$ Equation (1-13)

θ is the included angle of the propagate direction and z axis(light axis).

As a result, when light propagate in this medium, the two directions of propagations will have different propagate and phase velocities, and also phase retardations. Before the light passes through the medium, the two parts of light will combine together again.

Here are two examples:

I. When the direction of propagation along z axis(light axis):

Then θ will become 0, and substitute into Equation (1-12) and Equation (1-13).

We will get:

O wave : $n = n_o$ and E wave : $n(0) = n_o$

Since the two has the same phase velocity, $k_1 = k_2 = n_o(\frac{\omega}{c})$. After light propagate in this two modes for a distance d, from Equation (1-4), the light does not have phase retardation.

That means the polarization of light won't change.

II. When the direction of propagation along x-z plane:

From Equation (1-12) and Equation (1-13):

$$\text{O wave : } n = n_o \text{ and E wave : } n_e(\theta) = \left[\frac{\cos^2 \theta}{n_o^2} + \frac{\sin^2 \theta}{n_e^2} \right]^{-1/2}$$

$$\text{O wave has wave vector: } k_o = n_o \left(\frac{\omega}{c} \right) s \text{ ,}$$

$$\text{E wave has wave vector : } k_e = n_e(\theta) \left(\frac{\omega}{c} \right) s \text{ ,}$$

We can derive the phase transition for Equation (1-8), the light propagate in this medium for a distance d,

$$\text{O wave has a phase transition: } n_o \left(\frac{\omega}{c} \right) d \text{ ,}$$

$$\text{E wave has a phase transition: } n_e(\theta) \left(\frac{\omega}{c} \right) d \text{ ,}$$

the two has a phase retardation Γ :

$$\Gamma = [n_e(\theta) - n_o] \left(\frac{\omega}{c} \right) d \quad \text{Equation (1-14)}$$

Or

$$\Gamma = \frac{2\pi}{\lambda} [n_e(\theta) - n_o] d \quad \text{Equation (1-15)}$$

This phase retardation can generate a change of light polarization, from Equation (1-8). Light propagate in the liquid crystals will change the phase because of the phase retardation and causes different light intensity passes through. By controlling the liquid crystals to change the light intensity is also the main function uses in liquid crystal display.

(The derivation and formulas from Equation (1-2) to Equation (1-15) are come from the book "Elements of Photonics, Volume I: In Free Space and Special Media." [7])

1-3 SOME CHARACTERS AND STRUCTURE OF LCD

LCD is a kind of displays that uses liquid crystal to control the polarization of polarized light waves and form a display element. LC cell can make the light travel in a fixed direction. Since liquid crystals cannot emit light by itself, it needs a backlight. In the present market conditions, we often use CCFL and LED as the backlight. But they are not planar light, so they need ELP and diffuser to turn the point light or linear light into uniform planar light.

We also need polarizer and analyzer to polarize and examine the light. Polarizer can make the un-polarized light polarized in a fixed direction. Analyzer can only let the light has the same polarized direction as the analyzer's passes. As a result, analyzer affects the brightness of the display seriously.

LC cell includes ITO glass, alignment layer, LC, TFT (Thin Film Transistor), color filter, etc. ITO is a transparent conduct electrode, coated on the upper substrate and lower substrate. Besides, to maintain the alignment of the liquid crystals in the cell, we need an alignment layer (usually use polyimide) to hold them in the same position.

We will coat color filter on the upper substrate to have a full colored display and put TFT on lower substrate and supply the voltage for liquid crystal.

1-4 LCD OPERATION

Since liquid crystal would react different when different electric field is applied. We can divide them into two groups, normally white and normally black. When no voltage applied, we named the LC cell tends to have the bright state as normally white, and LC cell tends to have dark state as normally dark.

Take normally white TN cell as our example of LCD operation. When un-polarized light irradiate from the back light, it would pass a polarizer first, leave the light that has the same

polarized direction as polarizer's to enter the liquid crystal cell. When no electric field applied, there will be phase retardation and the bright state. When we applied an electric field on the LC layer, the liquid crystal's z axis would have the same direction with the electric field. The phase retardation would be zero and the light can't pass through the analyzer, and causes the dark state. We can modulate the electric field and LC cell like an optical-electrical control element to have the grayscale and light's brightness.

1-5 OPTICAL COMPENSATED BEND (OCB) MODE OF LC

The pi-cell is generally considered to be the fastest electro-optic response Nematic liquid crystal device [8], and improved to be optical compensated bend (OCB) liquid crystal display by an additional biaxial compensating film [9]. This kind of display aligns in splay state and operated in the bend state.

The device contains parallel-rubbed alignment layer and Nematic liquid crystal. It aligned in splay state and operated in the bend state. A nucleation process, takes a few seconds, is required before the pi-cell can become bend state and operate. The OCB mode devices has a response time around 5ms or even less, it's a faster switching time than conventional Nematic liquid crystal devices

1-6 MOTIVATION AND OBJECTIVE

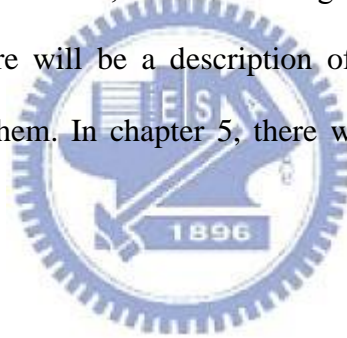
After P. J. Bos brought π cell out [8, 10] and Uchida brought bi-axial retardation film up to improve the dark state of pi cell, and named it as OCB cell [11, 12, 13]. We can apply the new mode in many applications since OCB has many advantages, for example, fast response time, low driving voltage, and wide viewing angle. It also can be used in high frequency

display products. Despite these many advantages, OCB mode needs to operate in bend state, and needs to apply a critical voltage to become bend state [14].

In this thesis, we use an additional layer made by Reactive Nematic liquid crystal Monomers to eliminate the critical voltage of OCB cell. Furthermore, we will observe the transmittance, retardation, and the pretilt angle of the new OCB cell.

1-7 ORGANIZATION OF THIS THESIS

In this thesis, we are going to present the detail of OCB cell, include function, character, and applications in Chapter 2. Chapter 3 will introduce some equipment that helps us to measure and evaluate the cell's condition, and fulfill our goal to eliminate the critical voltage of OCB cell. In chapter 4, there will be a description of the experimental processes and analyze the result and discuss them. In chapter 5, there will be a conclusion and expected future work.



CHAPTER 2

OVERVIEW OF OCB CELL

The optically compensated bend (OCB) cell [12,13,14], also known as pi-cell [9,10], has strengths of wide viewing angles[15] and fast response time[16] less than 3 ms since there is no backflow involved in its' switching. [17-20] Nevertheless, there are some drawbacks of OCB cell, for example, contrast ratio and phase pre-transition. OCB cells will initially stable at the splay state. The transition is needed to operate in the bend state. The voltage higher than critical voltage is required to transform the phase from splay state to bend state. Since the critical voltage will be different for R (red), G (Green), B (Blue), the three original colors, applying operation voltage bigger than all three critical voltages is essential for display application. Consequently, the transmittance has been sacrificed because of the need of large critical voltage. Some methods have been brought out to solve the issues, for example, using an electrical twist field in π cell [21] or polymer-stabilized walls [22-23] and increasing high pretilt angle [24]... etc. These methods, however, are quite different from conventional TN- or OCB-cell process.

2-1 THE CHARACTERISTICS OF OCB CELL

2-1-1 THE STRUCTURE OF OCB CELL

In Fig. 2-A, OCB cell's structure and five configurations are shown [25-27]. For an OCB cell, it usually consists of two ITO glasses as the upper and bottom substrates. The alignment layer on top of the substrate helps liquid crystals inside to align, and the pretilt angle is around 6 to 14 degree, such pretilt angle makes the LC molecules align in splay state in a plane without distortion. The normal state for OCB as a result will be splay state. When applied a voltage above the threshold voltage, the splay state would turn into symmetric splay state (also called Hs state) or asymmetric splay state (also called Ha state). When a voltage above the critical voltage applied, the cell would have a nucleation and change to bend state, that's where the liquid crystals were operated for OCB cell. After the applied voltage released, the cell would become 180° twist state first before it goes back to splay state.

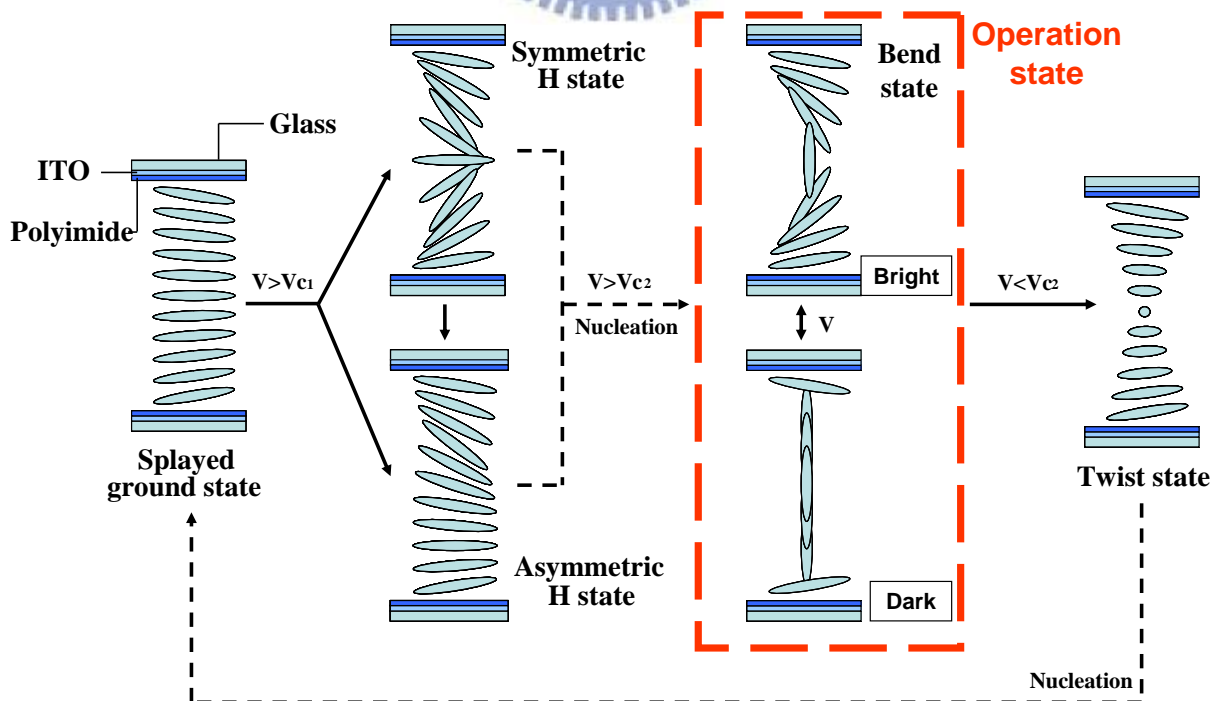


Fig. 2-A: OCB cell's structure and five configurations.

Hs state and Ha state is a transient state, when the tilt angle on both substrates is the identical, the cell would turn into Hs state, otherwise, the cell would turn into Ha state. V_{c1} in the figure usually would be $1V_{rms}$, and V_{c2} is around $2V_{rms}$ for most materials. The bend state is topologically different from splay state, that's the reason for a nucleation process and usually takes few seconds to minutes to complete the transition. The twist state to splay state process for conventional twisted nematic device usually takes longer than OCB cell because of the backflow-induced alignment phenomenon [28]. OCB cell has symmetry pretilt angle on each surface and causes the flow which produces no backwards torque on the director near the center of the cell, and eliminates the adverse effects of flow alignment. This phenomenon can be explained by Van Doorn [29] using the numerical solution of the Ericksen-Leslie equations [30]. Fig.2-B shows the torque which induces by the flow accelerates the relaxation.

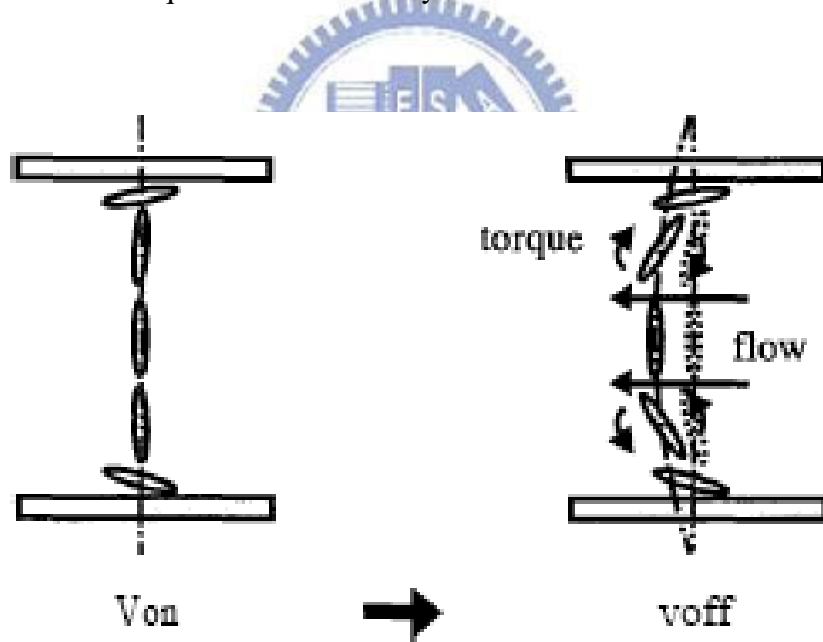


Fig. 2-B: Schematic figure of the dynamics in the pi-cell. The flow induces the torque to accelerate to relax. [31]

2-1-2 FAST RESPONSE

One of the famous advantages of OCB cell is fast response [32-33]. OCB cell operates in bend mode as Fig. 2-C (b) and homeotropic state as Fig.2-C (c) show. Since the alignment between these two states is alike, the response time is fast. Plus the no backward torque as mentioned earlier when removed the voltage, the response time is about 1 to 10ms, faster than TN mode (50 ms) and the response of human eyes (20 ms).

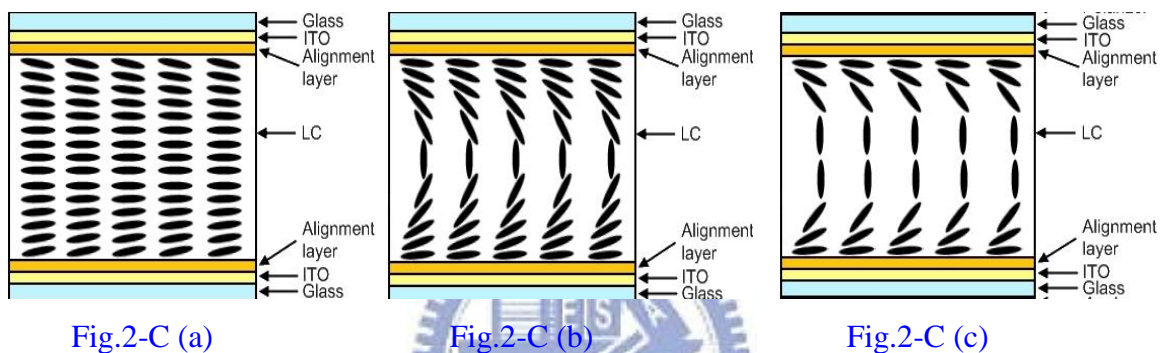


Fig. 2-C: (a) splay state, (b) V_{off} (V_{cr}), bend mode, and OCB cell is in the bright state. (c) V_{on} , homeotropic state, and OCB cell is in the dark state.

2-1-3 WIDE VIEWING ANGLE

Another advantage of OCB cell is wide viewing angle. From Fig. 2-D, compare TN mode with OCB mode, the transmittance is 50%, the curve of TN mode has asymmetric distribution, while the curve of OCB cell has symmetric distribution. TN mode LCD is difficult to compensate the birefringence because of the complicated alignment structure. From the cross-section view of OCB cell in Fig. 2-E, the alignment of LC molecules is symmetric in the vertical direction and experience the same optical path along the symmetric direction in this plane. There is self-compensated effect in this direction. Therefore, the horizontal viewing angle of π cell is wider and symmetric than TN mode.

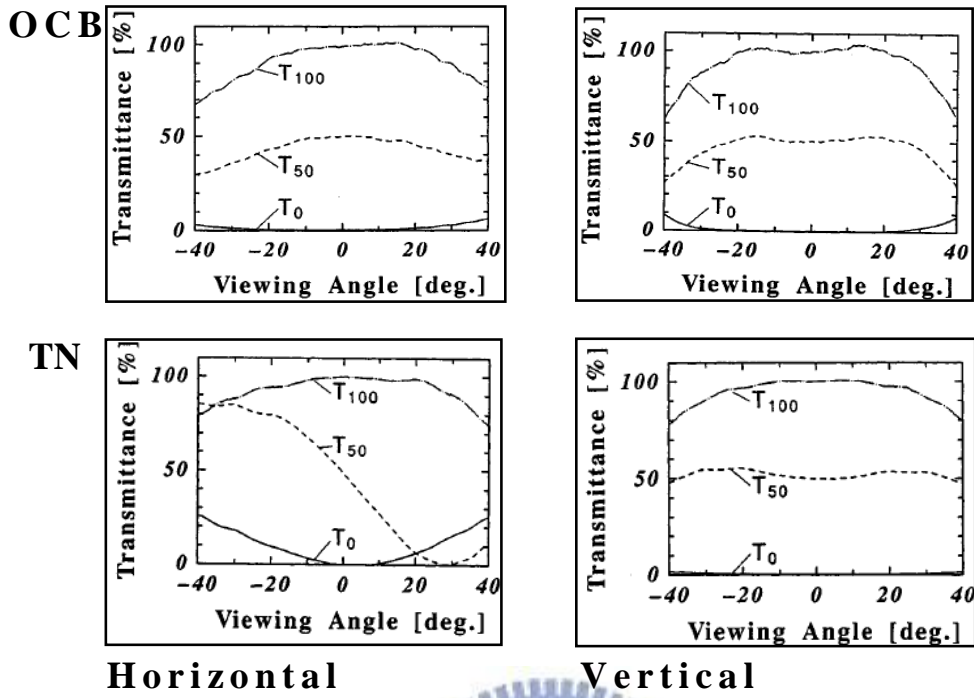


Fig. 2-D: Experimental results of the viewing-angle-dependent transmittance for TN cell and OCB cell [11].

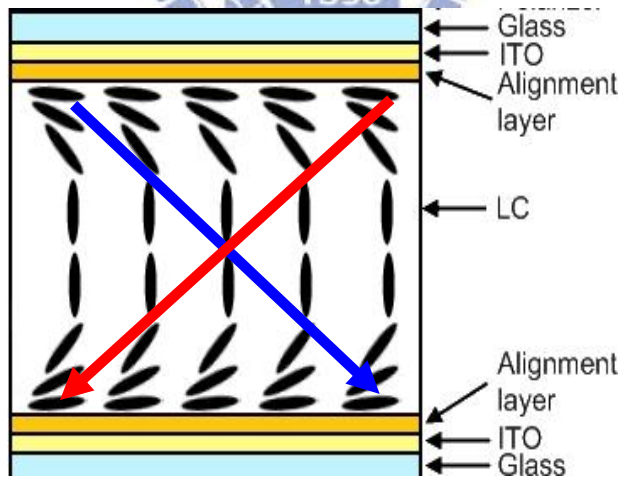


Fig. 2-E: cross-section view of OCB cell, it has symmetric viewing angle.

2-1-4 NUCLEATION AND PHASE TRANSITION

As mentioned in earlier section, when applying a high voltage to the OCB cell, the splay state would transit to bend state. It is found that the transition is divided into two stages [34]. Fig. 2-F explains the process. Because of the topologically difference between these states, the transition starts with breaking the anchoring symmetry at the cell surfaces and forming a bend domain with a disclination loop around it. It clearly demonstrates it in the simulation by P. J. Bos *et al.* [35]. The velocity of the disclination lines motion can be calculated from the energy difference of the two states. The energy difference of the two states can be obtained in a simple formulation, called Boundary-Layer Model [36-37]. The declination lines finally annihilate with each other when the transition is completed.

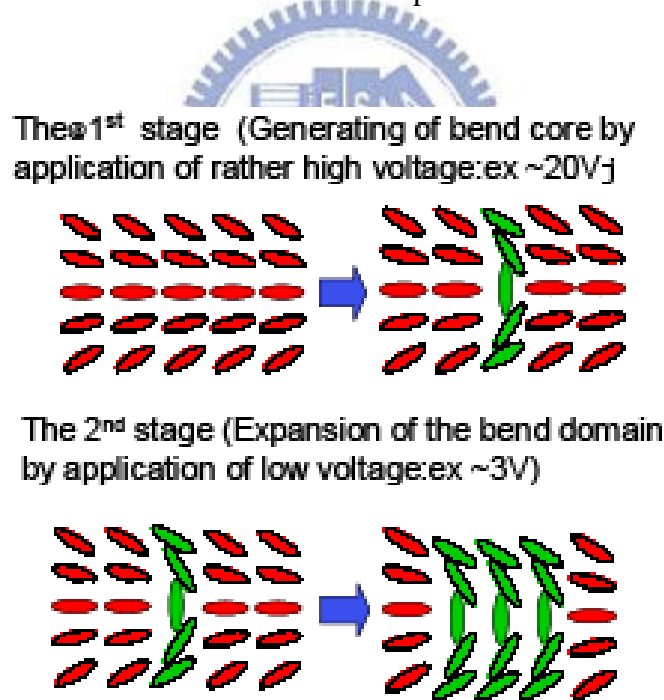


Fig. 2-F: Mechanism of bend transition [34].

Bend transition cores can be generated by defects and structures such as spacers [38]. When applied voltage, anisotropic structures around the spacers by adsorption are able to nucleate the bend state.

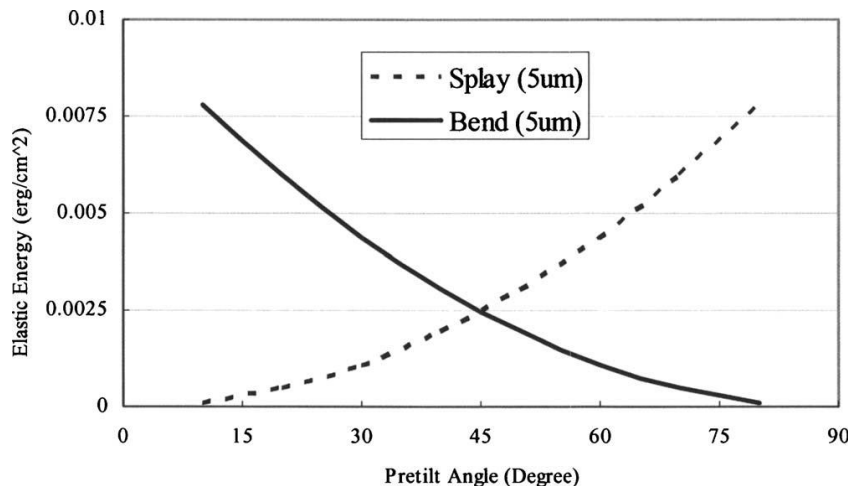


Fig. 2-G: The pretilt angle versus energy distribution of splay state and bend state.

In Fig.2-G, the relation between Elastic energy and pretilt angle are presented. From this point, when the pretilt angle is larger, the elastic energy of splay state and bend state will be closer [39-40] and become easier to transit or don't even need a transition. When the pretilt angle is around 45 to 50 degree, the energy of these two states is almost the same. Since the pretilt angle of conventional OCB cell is around 6 to 14 degree, the elastic energy is smaller than bend's. Applied voltage will change the original energy distribution like Fig. 2-H shows.

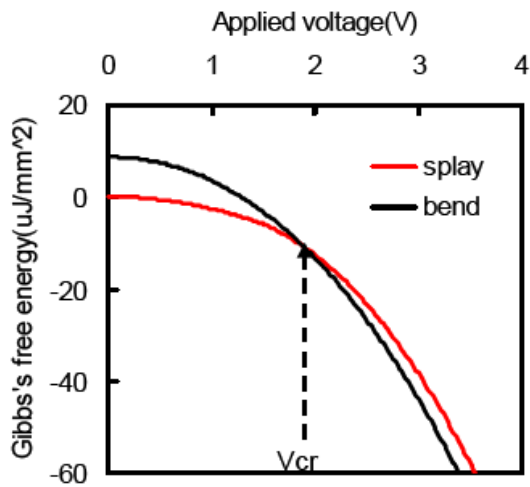


Fig. 2-H: Gibbs's free energy of bend and splay states as a function of applying voltage [34].

Therefore, we usually need to applied a voltage larger than critical voltage to the OCB cell for a while and wait the cell to transit to the higher energy bend state. It usually takes seconds to minutes to fulfill the process. The larger the voltage, the fast the process, however, too large voltage will not be suitable for TFT-drivers [41-42].

After the nucleation, the voltage corresponding to the 100% transmittance is called critical voltage (V_{cr}), and the voltage corresponding to the 0% transmittance is called dark state voltage, OCB cell usually operates between these two voltage.

Some methods have been brought out to solve the phase transition issue, in addition to those mentioned in the introduction, there are still some other examples like generate bend core or chiral dopant [43-44] or multi-dimensional alignment [45] and offer a twist electric field[46]...etc. These methods may shorten the transition time but sacrifice some innate advantages of OCB cell.



2-1-5 LIGHT LEAKAGE IN DARK STATE

The pretilt angle of OCB is usually around 6 to 14 degree. Compare to VA mode displays, the pretilt angle is 90 degree. When applied a voltage higher than critical voltage and make OCB cell become homeotropic or dark state, the liquid crystals near the substrates suffer huge constrained strength from the PI layer, and couldn't stand up like the VA mode displays. [Fig. 2-1](#) could explain the arrangement of VA and OCB mode. As a result, there will be a light leakage in the dark state. The contrast ratio will be lower than the VA mode, even with an additional compensation film. This phenomenon causes a weakness of OCB cell in the dark state.

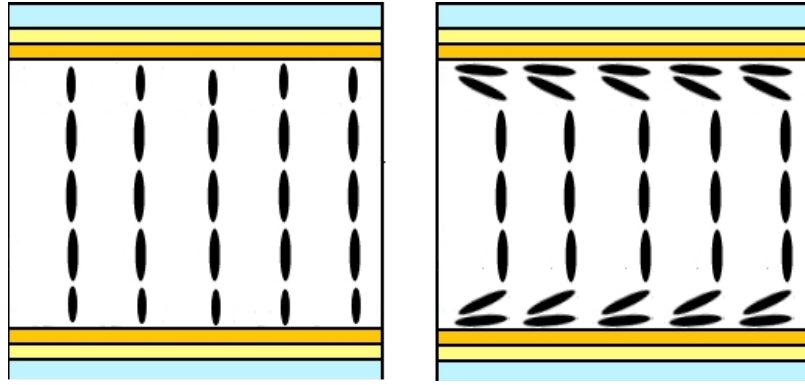


Fig. 2-I (a)

Fig. 2-I (b)

Fig. 2-I: The LC molecules alignment of (a) VA mode, and (b) dark state of OCB cell.

2-2SUMMARY

In this chapter, some of the details of OCB cell were introduced. OCB cell maintains many advantages, such as fast response time and wide viewing angle. Unfortunately, the fast response means operate in 'bend mode', and needs a phase transition to become bend mode. The transition time could be long if the driving voltage is low, but high voltage is not suitable for TFT-driving devices. On the other hand, the contrast ratio is poor than VA mode displays, and light leakage could cause power consumption waste. Based on the good side of OCB cell, it is worth to improve the OCB cell and make it more applicable for the liquid crystal display.

CHAPTER 3

MEASUREMENT SYSTEMS

The measurement systems that can help us get the E-O characteristics of the cell and the cell structures will be introduced in this chapter. The first one will be Atomic force microscope; it can help us to measure the thin film's thickness and surface condition. The second one will be UV/Vis spectrometer; this machine can help us measure the OCB cell's transmission spectrum and analyze the cell gap by interferometric method. The last but not least one will be the laser optical system; this one can measure the electro-optic characteristics and shows the relationship between voltage and cell's transmittance.

3-1 ATOMIC FORCE MICROSCOPE

The atomic force microscope (AFM) consists of a flexible micro-scale cantilever with a scanning sharp tip at its end that is used to scan the specimen surface, and use feedback mechanisms that enable the piezo-electric scanners to maintain the tip at a constant force. The cantilever is typically silicon or silicon nitride with a tip radius of curvature on the order of nanometers. The tips typically have an end radius of 2 nm to 20 nm, depending on tip type. When the tip is brought into proximity of a sample surface, forces between the tip and the

sample lead to a deflection of the cantilever according to Hooke's law. Depending on the situation, forces that are measured in AFM include mechanical contact force, Van der Waals forces, capillary forces, chemical bonding, electrostatic forces, magnetic forces, Casimir forces, solvation forces etc. Typically, the deflection is measured using a laser spot reflected from the top of the cantilever into an array of photodiodes.

The scanning motion is conducted by a piezoelectric tube scanner which scans the tip in a raster pattern with respect to the sample (or scans to the sample with respect to the tip). The tip-sample interaction is monitored by reflecting a laser off the back of the cantilever into a split photodiode detector. By detecting the difference in the photo-detector output voltages, changes in the cantilever deflection or oscillation amplitude are determined. The schematic diagram of this mechanism is depicted in Fig. 3-A (a) and (b).

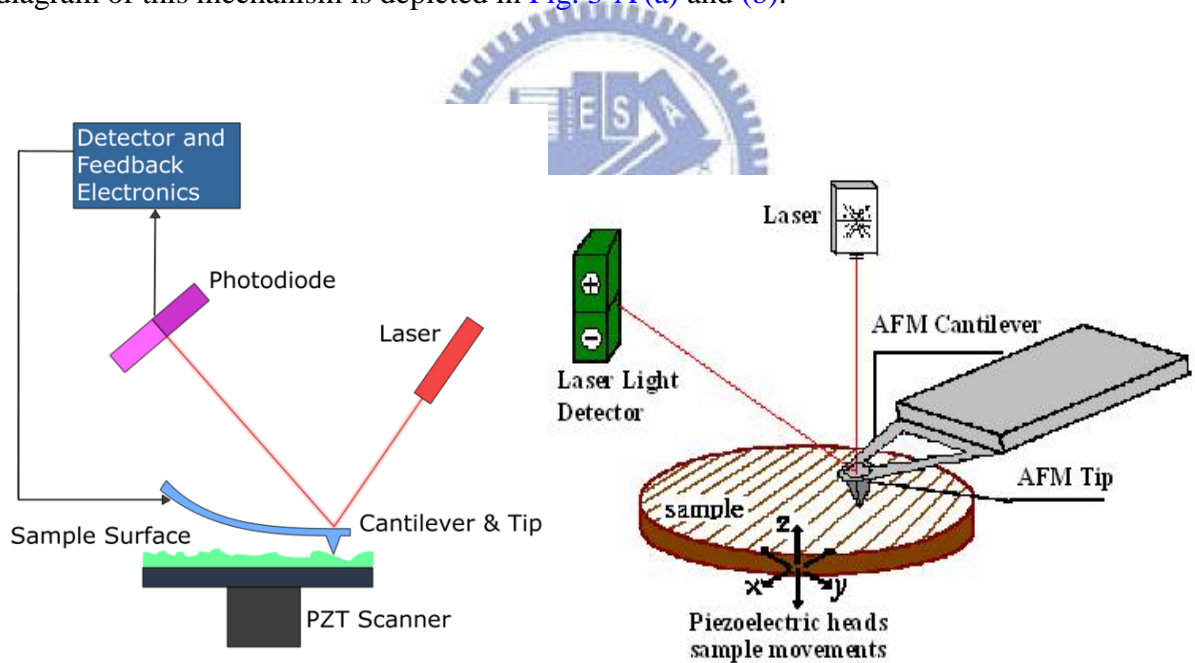


Fig. 3-A (a)

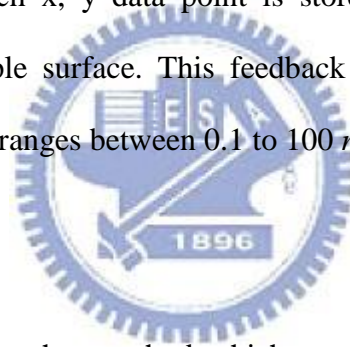
Fig. 3-A (b)

Fig. 3-A: (a) Block Diagram of Atomic Force Microscope (b) Concept of AFM and the optical lever.

There are 2 major operation modes for AFM :

I. Contact mode

Contact mode is the most common method to operate the AFM. But as the term suggests, the tip and the sample remain in close contact as scanning proceeds at this mode. One of the drawbacks of remaining in contact with the sample is that there exist large lateral forces on the sample as the tip is "dragged" over the specimen. It consists of scanning the probe across a sample surface while monitoring the change in cantilever deflection with the split photodiode detector. A feedback loop maintains a constant cantilever deflection by vertically moving the scanner to maintain a constant photo-detector difference signal. The distance the scanner moves vertically at each x, y data point is stored by the computer to form the topographic image of the sample surface. This feedback loop maintains a constant force during imaging, which typically ranges between 0.1 to 100 *nN*.



Non-contact mode

Non-contact operation is another method which may be employed when imaging by AFM. The cantilever must be oscillated above the surface of the sample at such a distance that we are no longer in the repulsive regime of the inter-molecular force curve. This is a very difficult mode to operate in ambient conditions with the AFM.

II. Tapping mode

It is the next common mode used in AFM. The cantilever is oscillated at its resonance frequency (typically ~300 *kHz*) and positioned above the surface so that it only taps the surface for a very small fraction of its oscillation period when operated in air or other gases. The laser deflection method is used to detect the root-mean-square (RMS) amplitude of cantilever oscillation. A feedback loop maintains constant oscillation amplitude by moving the

scanner vertically at every x, y data point. Recording this movement forms the topographical image. This is still contact with the sample in the sense defined earlier, but the very short time over which this contact occurs means that lateral forces are dramatically reduced as the tip scans over the surface. The advantage of tapping mode over contact mode is that it eliminates the lateral, shear forces present in contact mode, enabling tapping mode to image soft, fragile, and adhesive surfaces without damaging them, which can be a drawback of contact mode AFM. In this thesis, the tapping mode AFM was used.

The Contact Mode and Tapping Mode are the most common ones because it can conduct in air or liquid environments.

Using AFM has several advantages as follows:

First, the samples don't need any special treatments such as metal coating, etc before they viewed by AFM. That will be very convenient and need not to worry the surface might be damaged by the additional treatment.

Second, AFM can operate in ambient air or liquid environment perfectly. There is no need to change the environment into a specific condition.

Third, AFM can provide a higher resolution than SEM and provide 3 dimensional surface profiles. On the contrary, SEM can only provide image or projection in 2 dimensions.

There are several disadvantages, too. For example, the AFM image's maximum height is smaller than SEM's. Second, an incorrect choice of tip for the required resolution can lead to image artifacts.

3-2 CELL GAP MEASUREMENT SYSTEM

The sample's thickness matters a lot in liquid crystal display and in our research. Before filled in liquid crystal in our hollow samples, we need to use UV/Vis spectrometer LAMBDA 950 from Perkin Elmer to measure the spectra of the samples and calculate the thickness by

interferometric method [47].

LAMBDA 950 from Perkin Elmer, is shown in **Fig. 3-B**, can measure the spectrum from Ultraviolet light to visible light, and from 175nm to 900nm, with the resolution ≤ 0.17 nm, and the spectrometer features a double-beam, double monochromator, and ratio recording optical system.

For applications such as sun protection, reflectance properties of flat panel display screens, paint films, transmission and reflectance characterization of glass and solar cells.



Fig. 3-B: UV/Vis spectrometer LAMBDA 950 from Perkin Elmer

As for the interferometric method, some basic concepts are introduced as follows.

For interferometric method, we need two reflective surfaces, as shown in **Fig. 3-C**. R1 is the reflective index of surface 1 and R2 is the reflective index of surface 2. When incident light passes through surface 1 and 2, there will be an interference of light.

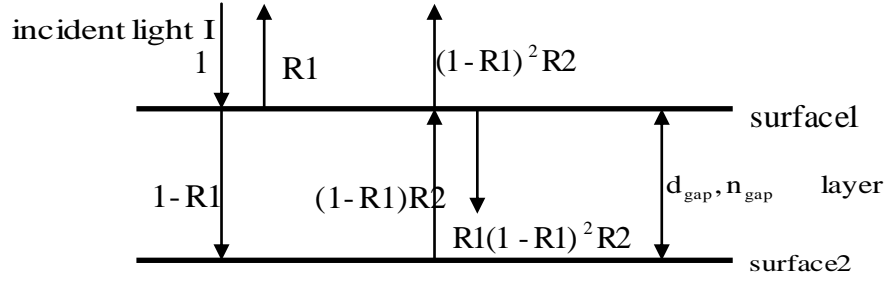


Fig. 3-C: Two surfaces possess reflective index R_1 and R_2 , light would pass through surface 1 and 2 and causing a light interference.

If total incident light is $I = \cos(\omega t)$ and assume no absorption of light in surface 1 and 2, then the total reflected light R can be written as Equation (3-1):

$$R = R_1 \cos \omega t + \sum_{k=1}^{\infty} R_1^{k-1} R_2^k (1 - R_1)^{1+k} \cos \omega(t - kt_0) \quad \text{Equation (3-1)}$$

$$t_0 = 2d_{\text{gap}} n_{\text{gap}} / c \quad \text{Equation (3-2)}$$

$$\omega = 2\pi c \sqrt{n_{\text{gap}}} / \lambda \quad \text{Equation (3-3)}$$

Where c is the speed of light in vacuum, λ is the wavelength, d_{gap} is the thickness of the layer, and n_{gap} is the refractive index of the layer.

The cosine factor k represents internal reflections for $k > 1$, and the internal reflections can be neglected since the magnitude of $k > 1$ when R_1 and R_2 will be smaller than 1 is much smaller than $k = 0$. Therefore the Equation (3-1) can be rewritten as Equation (3-4):

$$R = R_1 \cos \omega t + (1 - R_1)^2 R_2 \cos \left(\omega t - \frac{4\pi n_{\text{gap}} d_{\text{gap}}}{\lambda} \right) \quad \text{Equation (3-4)}$$

Thus the reflected spectrum is

$$|R(\lambda)|^2 = R_1^2 + [(1 - R_1)^2 R_2]^2 + 2R_1(1 - R_1)^2 R_2 \times \cos(4\pi n_{\text{gap}} d_{\text{gap}} / \lambda) \quad \text{Equation (3-5)}$$

The periodic term in Equation (3-5) causes an interference pattern. The periodicity of the reflected interference spectrum determined the optical thickness of the cell gap, n_{gap} and d_{gap} .

If λ_1 and λ_2 are the two wavelengths showing extrema in Equation (3-5), then we can derive Equation (3-6), (3-7), (3-8) for $\lambda=\lambda_1$ and $\lambda=\lambda_2$.

$$\cos(4\pi n_{gap} d_{gap} / \lambda) = \pm 1 \quad \text{Equation (3-6)}$$

$$2n_{gap} d_{gap} = k_1 \lambda_1 / 2 \quad \text{Equation (3-7)}$$

$$2n_{gap} d_{gap} = k_2 \lambda_2 / 2 \quad \text{Equation (3-8)}$$

Where k_1 and k_2 are natural numbers.

Suppose $\lambda_1 > \lambda_2$, then for x is a nature number, k_2 can be presented as Equation (3-9).

$$k_2 = k_1 + x \quad \text{Equation (3-9)}$$

Based on Equation (3-7), (3-8), and (3-9), we can write

$$n_{gap} d_{gap} = \frac{x \lambda_1 \lambda_2}{4(\lambda_1 - \lambda_2)} \quad \text{Equation (3-10)}$$

The value of $x-1$ indicates the number of extrema in $|R(\lambda)|^2$ between the wavelengths λ_1 and λ_2 . It is better to choose the distance x between the two extrema as large as possible to improve the preciseness of the calculation of $n_{gap} d_{gap}$. We present a sample's result measured by UV/Vis spectrometer LAMBDA 950 as an example, the spectrum is shown in Fig.3-D.

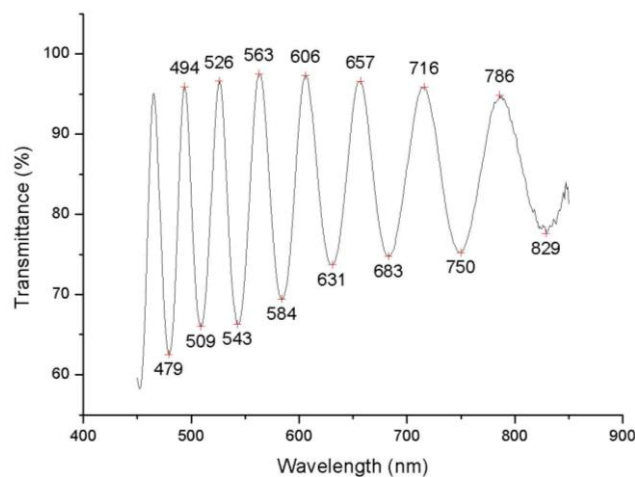


Fig. 3-D: The spectrum result for the sample as an example.

From the figure, the sample has the following parameters, $\lambda_1=786$, $\lambda_2=494$, $x=12$, and the result is shown in Equation (3-11)

$$n_{gap} d_{gap} = \frac{x\lambda_1\lambda_2}{4(\lambda_1 - \lambda_2)} = \frac{12 \cdot 786 \cdot 494}{4 \cdot (786 - 494)} = 3.98 \mu\text{m} \quad \text{Equation (3-11)}$$

3-3 LASER OPTICS SYSTEMS

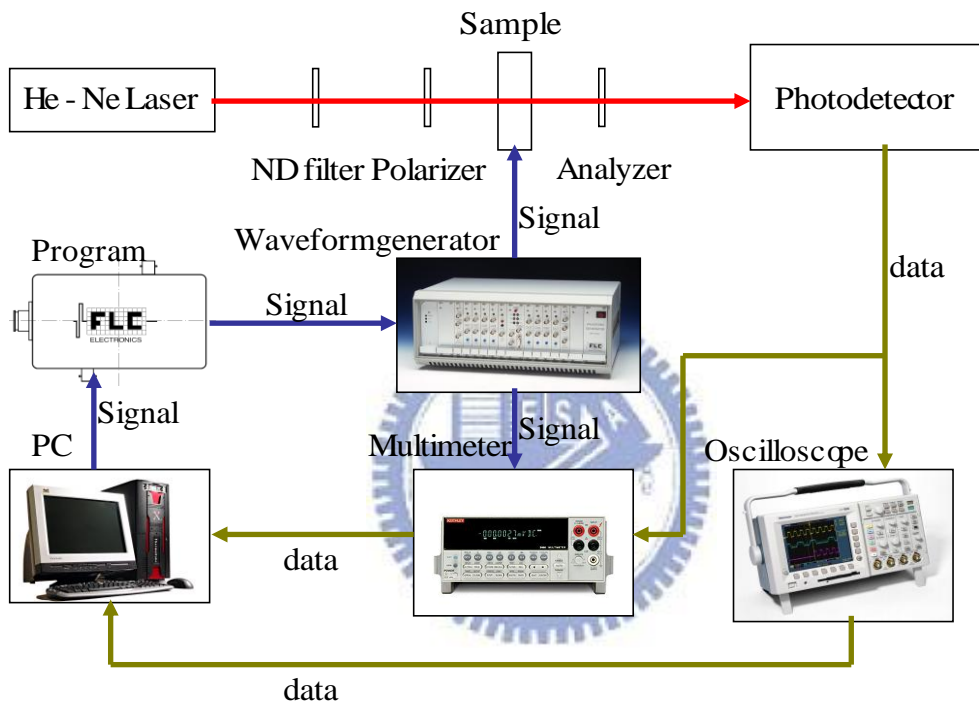


Fig. 3-E: the scheme of laser optic system.

We use laser optic system show as Fig.3-E to measure the electro-optic characteristics of our RMM-OCB cell. The major measurements include Voltage versus Transmittance, retardations, and response time.

We use He-Ne laser with wavelength equals 632.8nm as our laser source. After we put our sample in the middle of polarizer and analyzer, the laser would pass a 10% ND filter first to degrade the intensity into an acceptable range for photo detector. Then the laser would travel trough the polarizer, cell, analyzer, and finally to the photo detector. The laser light

would become a polarized light after passed through the polarizer. Based on the birefringence characteristic of liquid crystals, it possesses a Δn when light passes through and causes retardation, like a phase modulator. The polarized laser light would pass through the liquid crystal cell and change the phase depend on $2\pi\Delta nd/\lambda$. Finally, the polarized light would pass through the analyzer and received by the photo detector. The photo detector PIN20 (from FLC Electronics AB) can detect any signal with its response more than 40ns. Then the oscilloscope (from Tektronix) would get the signals and digitized it and read by a Signal Multimeter (from Keithley), and then transfer the signals to the PC.

WFG500 (from FLC electronics AB) is a multi-channel high voltage waveform generator. The range for the maximum output voltage is $\pm 100V$ and the minimum designable pulse width is 200ns. We also wrote a program called ‘FLC’ to drive the LC cell by WFG500 (from FLC electronics AB) and connected with PC through GPIB interface. The frequency and waveform applied to the cell will be 1k Hz square wave for the voltage versus transmittance measurement.

When measuring the retardation of the cell, a compensator (Soleil-**Babinet**, From Special Optics, Model:8-400-UNCOATED) would be put in the middle of polarizer and analyzer, like Fig.3-F. We would rotate the compensator and record the two minimum signals detected by photo detector, and set them as min_1 and min_2 .

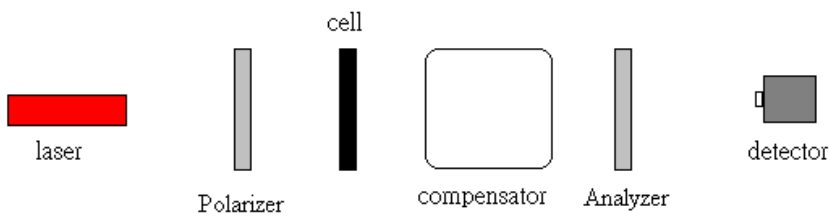
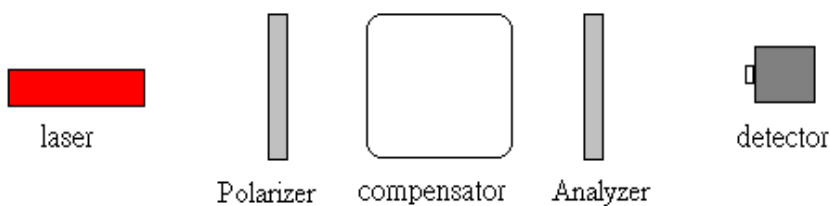


Fig.3-F (a): the installation of retardation measurement. Fig.3-F (b): LC cell position.

The cell would be put in the middle of polarizer and compensator like Fig. 3-F (b), and rotate the compensator to record the minimum signal 'x' that detected by photo detector. By substitute the 'x' value into Equation (3-12) we can get the retardation value.

$$\text{Retardation value} = \Gamma = (x - \min_2) \div (\min_1 - \min_2) \quad \text{Equation (3-12)}$$

Moreover, with Equation (3-13) as followed, d means cell gap or film's thickness, we can even derive the cell's Δn with cell gap (d) or opposite.

$$\text{Retardation value} \times \frac{2\pi}{360} = \frac{2\pi}{\lambda} \times \Delta n \times d \quad \text{Equation (3-13)}$$

$$\rightarrow \Delta n = \frac{\text{retardation value} \times \lambda}{360 \times d} \quad \text{Equation (3-14)}$$

3-4 POLARIZED OPTICAL MICROSCOPE (POM)



Fig. 3-G: the picture of POM.

The polarized optical microscope (POM) *Olympus BX51* is designed to observe and photograph specimens that are visible primarily due to their optically anisotropic characteristic. Besides, transparent and reflective specimens can both be observed by this POM. In this instrument, the light would travel through a polarizer before it passes the specimens, and then an analyzer. Optical images will be monitored with a charge-coupled device (CCD) camera connected to a Personal computer. We have different choices on the magnifications and object lens, 100x, 200x, 500x, and 1000x for the first one, and 10x,20x,50x,and 100x for the second one, and a 10x for the ocular lens.



CHAPTER 4

EXPERIMENTS AND RESULTS

In application, OCB cell has two main advantages that degrade its performance, first one will be critical voltage's existence and the second one is insufficient dark state. OCB cell needs a high pulse voltage to transit its splay state into bend state to operate, and the alignment of OCB cell has more light leakage than other liquid crystal cells, for example, TN, VA, and IPS. Insufficient dark state will cause the contrast ratio inadequate, too.

In this essay, an additional layer made by nematic acrylate mixture (also called RMM-19B, from Merck Co.) were coated on top of the PI layer and formed a higher pretilt angle. Since the pretilt angle has a negative relationship with the transition voltage [48], the transition voltage can be removed successfully. Moreover, the additional RMM layer can make the dark state darker than before. The details will be discussed later in this chapter.

4-1 CELL FABRICATION PROCESS

Fig. 4-A shows the procedure of OCB cell's fabrication:

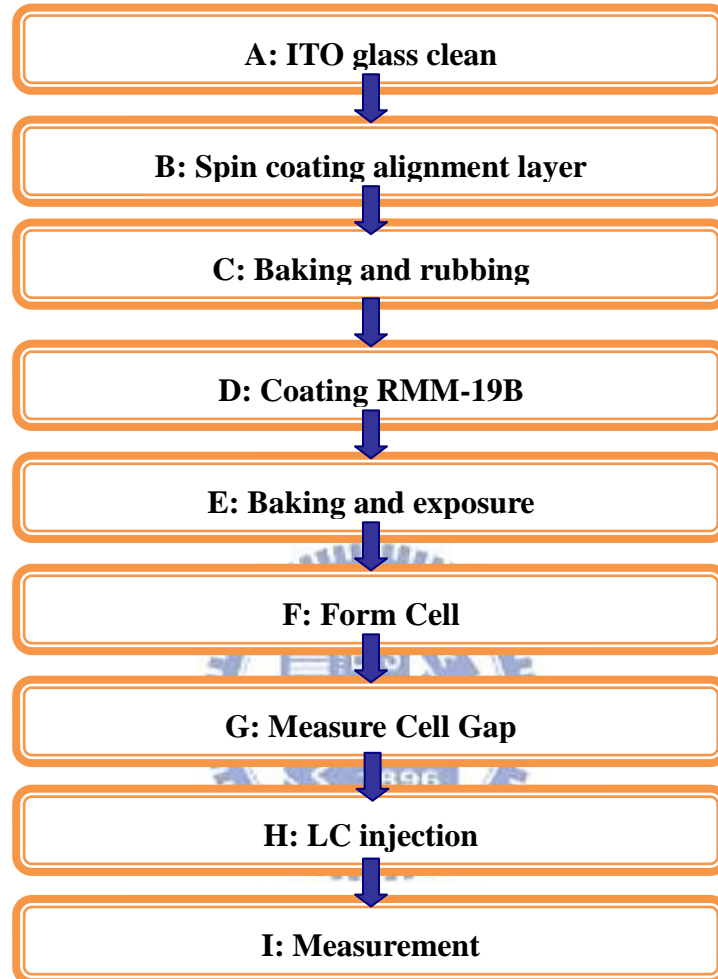


Fig. 4-A: Fabrication process of OCB cells.

A. The glasses that been used in this thesis are all pre-coated by Indium-Tin-Oxides (ITO) to make the glasses conducted. After cut the ITO glasses into small pieces of glasses that have $2\text{cm} \times 2.5\text{cm}$ areas, 5wt% detergent solution are been used to clean the glass's surfaces. This process usually took an hour and an half for 20 small pieces of glasses. Afterward, the clean glasses will be put into a supersonic cleaner for 30minutes. To dry off the glasses, Nitrogen will be used to blow over the surfaces first, and then baked for 1 hour.

B. A solution that compound with polyimide (Chisso PIA-5580-01) and solvent were made. The ratio of the mixture solution will be PI: Solvent equals 3:1. The pretilt angle of the polyimide is around 7°. In the same time, the dry ITO glasses will be put into an UV-Ozone for 20 minutes to increase the hydrophile of the surfaces. After that, the mixture solution were filled into a glass syringe and put on a 0.2um filter to leach extra particles. Then drip the mixtures on glasses and use a spin coating machine to create the uniformity of the polyimide. The parameters of the spin coating are given as [Table 4-A](#).

Table 4-A. Parameters of spin coating polyimide		
	Speed	Time
Solvent-Waiting	0rpm	30secs
Solvent-1 st spin	800rpm	30secs
Solvent-2 nd spin	5000rpm	60secs
Polyimide mixture solution-Waiting	0rpm	30secs
Polyimide mixture solution -1 st spin	800rpm	30secs
Polyimide mixture solution -2 nd spin	5000rpm	60secs

C. After the glasses with PI on the surfaces were backed 220°C 1 hour. Rubbing machine with the following parameters ([Table 4-B](#)) will be rubbed on the sample glasses.

Table 4-B. Rubbing Conditions for Polyimide glasses	
Pile impression	0.2mm
Rotation speed	500rpm
Advancing speed	7.3mm/s

D. The following step is coating RMM-19B (from Merck Co.) on the PI layer. RMM-19B is in solid state when in room temperature. After dissolved the RMM-19B into PGMEA and make 2 different concentrations to do the experiment, 1st one is 2wt%, 2nd one is 4wt%. The results of 2wt% are not good as the 4wt% one, so the following results are going to discuss the 2nd concentration only.

Again, the glass syringe and 0.2um filter was used. Then RMM-19B will be dripped on the PI layer, and use a spin coating machine to create the uniformity of the RMM layer. The parameters of the spin coating are given in [Table 4-C](#).

Table 4-C. Parameters for RMM-19B				
	Time	Speed		
1st spin	30s	500rpm		
2nd spin	60s	Sample-1 & cell-1	Sample-2 & cell-2	Sample-3 & cell-3
		6000rpm	4000rpm	2000rpm

E. After coating, the sample were backed with 40°C to 50 °C and exposed to an UV light in the same time for 5 to 10 minutes to solidify the RMM layer.

F. The novel RMM cell structure has two different attempts in the substrate choices, the substrates with only PI on it or the substrates with additional RMM layer on top of the PI layer. The first type, called RMM-OCB cell, used only PI layer on it as the upper substrate and additional RMM layer as the bottom substrate. The second type, called RMM2-OCB cell, used additional RMM layer on both bottom and upper substrates. The types can be interpreted by [Fig. 4-B](#).

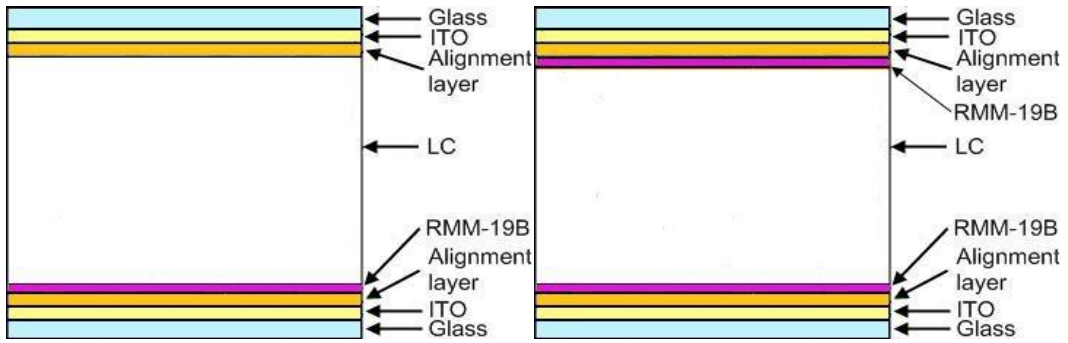


Fig. 4-B (a)

Fig. 4-B (b)

Fig. 4-B the two different types: (a) only the bottom substrate uses RMM layer glasses. (b) Both substrate use RMM layer on it.

Additionally, the spacer that used to seal the cells were mixed with UV glues (NOA-65, from Norland). For both cell types, we fabricated with two different spacers, $3.5\mu\text{m}$ and $5\mu\text{m}$. After sealed with spacer mixtures and exposed to UV lamp for 5 minutes. The cells are read to measure the cell gaps by spectrometer.

G. The cell gap of the empty cells was measured by UV/Vis spectrophotometer Lambda 950 (from Perkin Elmer). The machine's faculty has been explained in the previous chapter completely.

H. Afterward, the nematic liquid crystal, ZCE-5096XX (from Chisso), was injected into the cell by capillarity. The details of the liquid crystal were given as Table 4-D.

Table. 4-D. The parameters of liquid crystal ZCE-5096XX	
Sample	ZCE-5096XXXX
$T_{N \rightarrow C[S]}$	$< -20\text{ }^\circ\text{C}$
$T_{N \rightarrow I}$	$95.5\text{ }^\circ\text{C}$
Viscosity η (at 20°C)	$46.7\text{ mPa} \cdot \text{s}$

Table. 4-D. The parameters of liquid crystal ZCE-5096XX (conti.)		
Optical anisotropy (at 25°C 589nm)	Δn	0.158
	n_e	1.662
	n_o	1.504
Dielectric anisotropy (at 25°C)	$\Delta \epsilon$	10.0
	$\epsilon_{ }$	14.1
	ϵ_{\perp}	4.1
Specific resistivity ρ (at 25°C)		$>1.5 \cdot 10^{14} \Omega \cdot \text{cm}$
K_{11}		9.8 dyne
K_{22}		5.8 dyne
K_{33}		11.8 dyne
γ_1		178 mPas

- I. After soldered conducted wires on surface, the different types of cells were be able to measure the E-O characteristics.

4-2 CHARACTERISTICS OF REACTIVE NEMATIC LC MONOMERS

The reactive nematic liquid crystal monomers (from Merck Co.), also called RMM-19B or RMM for short, is a polymerizable nematic acrylate mixture, and was given a splay alignment. The mixture contains LC molecules and polymerization monomers that can be polymerized by UV irradiation or UV light exposure and became solidify on the surface. Since RMM-19B is also a LC material which provides phase retardation of linearly polarized light.

4-3 NOVEL OCB-CELL MODEL

The novel cell structure has RMM layer on top of the PI alignment layer. The RMM-OCB cell (first type) structure was shown in Fig. 4-C. From the figure, the additional RMM layer was able to achieve a higher pretilt angle on the substrate. As a result, a transition free OCB cell was obtained with high surface pretilt angle on the substrate [49-50]. Moreover, the RMM layer with residual retardation and easily aligned vertically at high voltage could improve the cell's contrast ratio. The novel structure can solve the phase transition issue and the drawback of contrast ratio at the same time.

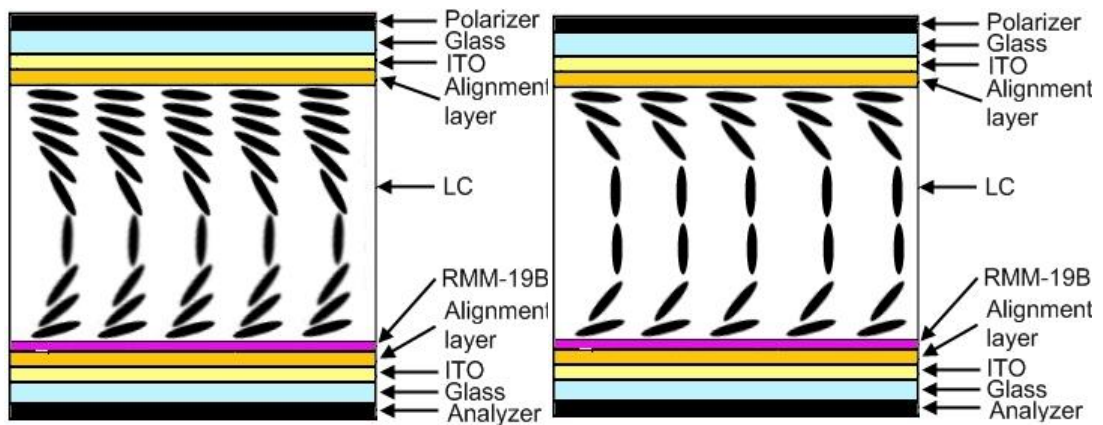


Fig.4-C (a)

Fig.4-C (b)

Fig.4-C The scheme of RMM-OCB cell under (a) 0V, (b) 6V

In order to know the uniformity and thickness of the additional RMM layer, AFM and polarizing optical microscope (also called POM for short) were used. In Fig. 4-D and Table.4-E, the uniformity and the thickness of the RMM layer were measured by AFM. The dark and bright state were measured by POM and showed in Fig. 4-E. From AFM and the pictures taken by POM, RMM-19B has good uniformity on top of the PI layer.

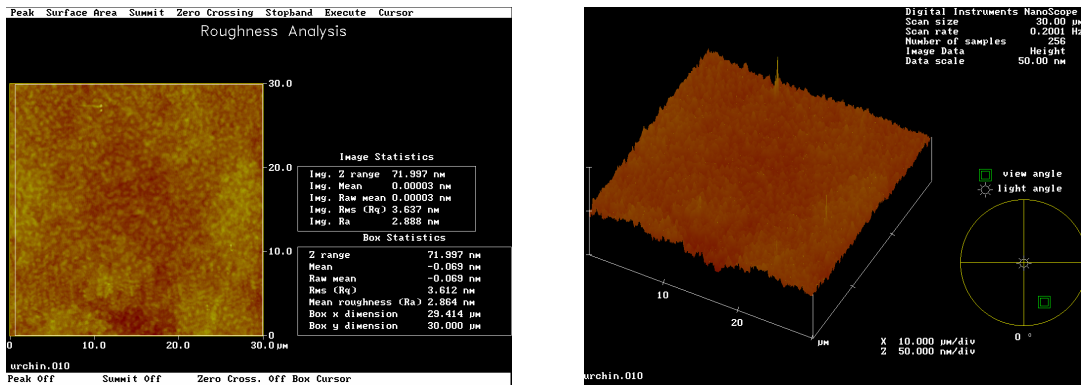


Fig. 4-D: RMM-19B microscopic structure observed by AFM. RMM-19B forms a thin film about 100~200 nm with 3 nm roughness.

Table. 4-E: RMM thickness with spin coating speed's relation				
Spin Coating Speed	6000 rpm	4000 rpm	2000 rpm	500 rpm
RMM thickness	80nm	110nm	134nm	200nm

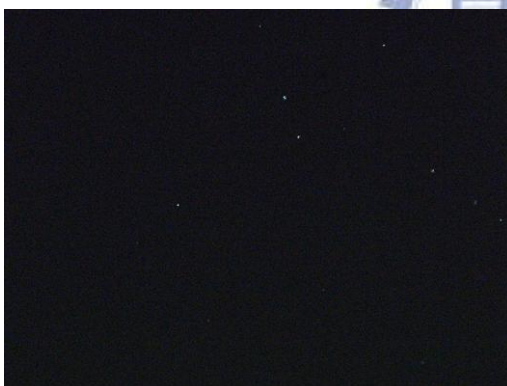


Fig. 4-E (a)

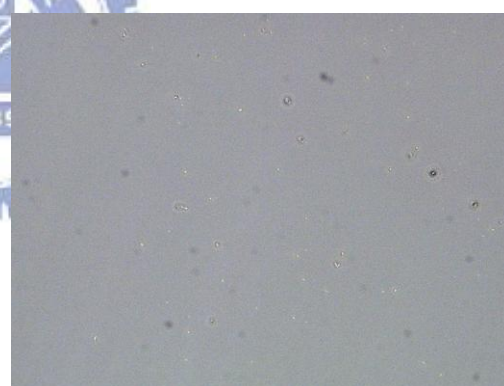


Fig.4-E (b)

Fig. 4-E: The pictures of RMM-19B when in (a) dark state and (b) bright state

4-4 MEASUREMENT OF ELECTRO-OPTICAL PROPERTIES AND RESULTS

4-4-1 PHASE TRANSITION FREE OCB CELL

The RMM-OCB cell that only has bottom substrate with additional RMM layer on it got the following results. If the cell gap of RMM-OCB cell is around or larger than 5 μm , there will be no phase transition when RMM layer is thicker than 130 nm. As for cells with cell gap equals 3 μm , all of them are transition free. The relationship between RMM layer's thickness and critical voltage were examined by AFM and the results are showed in Fig. 4-F. The thickness of PI layer is around 75 nm.

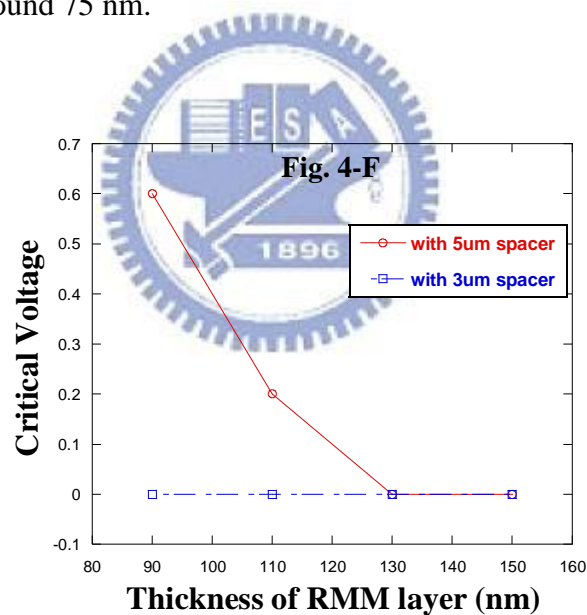


Fig. 4-F: the relation between the RMM layer's thickness and the cell's Critical voltage corresponds to different spacers.

From the figure, for cell's cell gap equals or bigger than 5 μm , the critical voltage will decrease while the RMM layer's thickness increases. Nevertheless, for those RMM-OCB cells have cell gaps equal or less than 3 μm , they were able to be driven without the phase

transitions. As for the relation between critical voltage with the spacers and with the thickness, the data is summarized in **Table.4-F** and **Table.4-G**. The RMM-OCB cell were put in the middle of the polarizer and analyzer in the laser optical system to measure the transmittance and V-T curve, like **Fig. 4-G**, the θ will be 45° .

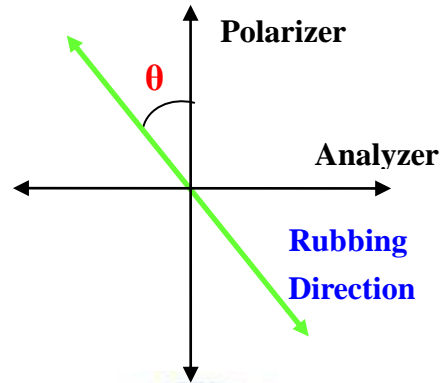


Fig. 4-G: the include angle $\theta=45^\circ$ between RMM-OCB cell's rubbing direction and polarizer's direction.

Table. 4-F: 4wt% RMM-OCB cells and conventional OCB cell-1 (cell gap $\sim 5.0\pm 0.05\mu\text{m}$)

Cell name	OCB	Cell-1	Cell-2	Cell-3
RMM thickness	None	90nm	110nm	134nm
Critical voltage	1.6V	0.6V	0.2V	0.0V

*without using compensation films, OCB means conventional OCB cell

Table.4-G: 4wt% RMM-OCB cells and conventional OCB cell-2 (cell gap $\sim 3.2\pm 0.05\mu\text{m}$)

Cell name	OCB	Sample-1	Sample-2	Sample-3
RMM thickness	None	90nm	110nm	134nm
Critical voltage	1.6V	0.0V	0.0V	0.0V

*without using compensation films, OCB means conventional OCB cell

The V-T curves in **Fig. 4-H (a)** and **Fig. 4-H (b)** are corresponded to 5 μm and 3 μm cell gaps. From **Fig. 4-H (a) & (b)**, the dark state of RMM-OCB cells are darker than the conventional OCB cell. In other words, the RMM-OCB cell suppressed more light leakage at oblique incidence than conventional one. As a result, the contrast ratio had improved greatly.

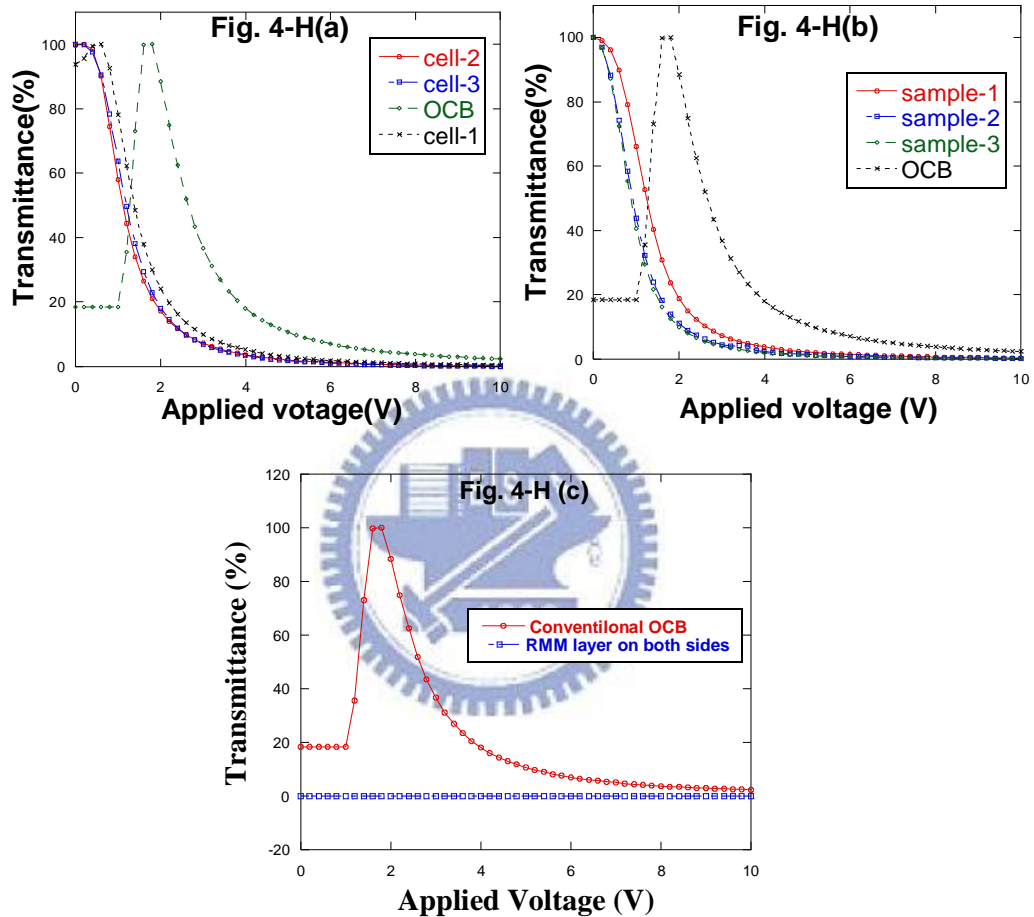


Fig. 4-H: Different thickness of RMM layers with (a) cell gap around 5 μm , and (b) cell gap around 3 μm , and (c) RMM layer on both substrates.

On the contrary, when measuring RMM2-OCB cell's transmittance and put the cell in the laser optic system, too. The system cannot let any light pass through and got nothing on the V-T measurement. The results are presented in **Fig. 4-H (c)**. This result pointed out the pretilt angle on the additional RMM layer may be high enough and causes liquid crystals inside

became homeotropic. The calculation of RMM layer's pretilt angle will be shown later in this chapter. To prove the homeotropic state in RMM2-OCB cell, the include angle ' θ ' between cell rubbing direction and the polarizer were changed and measured the transmittance in the same time. The results are presented in Table.4-H. From the results, the liquid crystals inside RMM2-OCB cell are in homeotropic state.

Table. 4-H: the transmittance of RMM2-OCB cell when in different include θ								
Angle(θ)	0	30	45	90	120	150	180	270
transmittance	0	0	0	0	0	0	0	0

4-4-2 RETARDATIONS

The retardations of both RMM-OCB cells and conventional OCB cell were measured by He-Ne laser ($\lambda=632.8\text{nm}$). As shown in Fig. 4-I, the conventional OCB cell has a similar retardation curve compared with RMM-OCB cell when the driving voltage was higher than critical voltage.

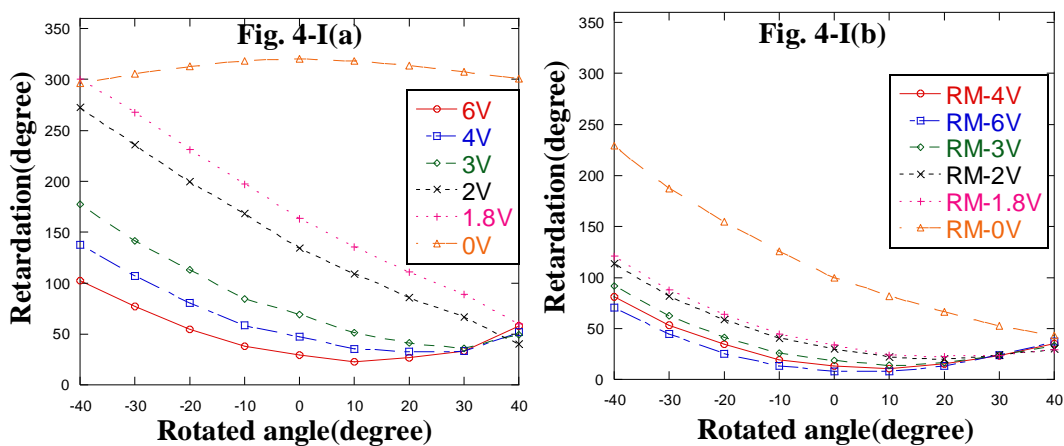


Fig.4-I (a) is conventional OCB cell's retardation. Fig.4-I (b) on the right is retardations of the RMM-OCB cells under applied voltage from 0V to 6V with different viewing angle.

This result suggested that the LC were arranged in the bend state when the applied voltage was zero in RMM-OCB cells. Comparing the dark state of the conventional OCB cell with the RMM-OCB cells, the retardations of RMM-OCB cells corresponding to different viewing angles were lower than the conventional OCB cell's. Moreover, the symmetry of the viewing angles of the RMM-OCB cells was better than the conventional one. The retardation curves were more symmetric than the normal direction viewing angle.

4-4-3 RMM SURFACE TILT ANGLE

To estimate the pretilt angle of the RMM layer, we performed the following experiments to do the evaluation. First, a thin (1.55 μm) homotropic RMM cell was prepared to get the retardation (at $\lambda=452\text{nm}$) of the RMM 19B. From Equation (4-1), we can get Δn of RMM material by measuring the retardation of homotropic aligned RMM cell. In order to simplify the calculation, we assumed uniform average LC tilt angle for RMM 19B film instead of splay orientation. Applying Equation (4-2) and (4-3), the tilt angle θ can be calculated from measured thin film retardation.

$$\Gamma = \frac{2\pi\Delta nd}{\lambda} \quad \text{Equation (4-1)}$$

$$\Delta n(\theta) = n_e(\theta) - n_o \quad \text{Equation (4-2)}$$

$$\frac{\cos^2\theta}{n_e^2} + \frac{\sin^2\theta}{n_o^2} = \frac{1}{n_e(\theta)^2} \quad \text{Equation (4-3)}$$

By assuming $n_o=1.52$, we can get n_e of the RMM material. Based on the assumption mentioned above, we can get $n_e(\theta)$ and infer the average pretilt angle of RMM-OCB cell. The data is summarized in [Table.4-I](#) and [Table.4-J](#).

Table.4-I: FLC-RMM cell, Δn of RM when $\theta=0$		
Cell gap	Δn	n_e
1.55μm	0.1176	1.6376

Table.4-J: Δn of RMM-OCB cell and pretilt angle			
Cell	Thickness	Δn	pretilt
Cell-A	237nm	0.0004	86.48°
Cell-B	120nm	0.0012	83.93°

From the calculation, RMM-OCB cell's average pretilt angle was around 78° to 87°. This estimation proved that the surface tilt angle is greater than 46° which is stable in bend configuration [51].



4-4-4 CONTRAST RATIO

The low contrast ratio is also a major drawback of OCB. The dark state is not dark enough, especially at oblique incidence. Generally, the LC molecules of the OCB cell are arranged vertically at the dark state; however, the LC molecules of the boundaries of the OCB cell cannot be perfectly vertical. In addition, the optical axis of the LC cell has a 45 degree diverged from the absorption axis of the polarizer, that causes a high optical retardation and increase the light leakage at the dark state. On the contrary, by using RMM modified cell, the data were summarized in [Table.4-K \(a\) & \(b\)](#).

Table. 4-K(a): contrast ratio of RMM-OCB cells and conventional OCB cell-1				
Cell name	OCB	Cell-1	Cell-2	Cell-3
RMM thickness	None	80nm	110nm	134nm
Critical voltage	1.6V	0.6V	0.2V	0V
Contrast ratio	26.4	123	224	272.6
Dark state(8V)	3.79	0.82	0.45	0.37

Table.4-K(b): contrast ratio of RMM-OCB cells and conventional OCB cell-2				
Cell name	OCB	Sample-1	Sample-2	Sample-3
RMM thickness	None	80nm	110nm	134nm
Critical voltage	1.6V	0V	0V	0V
Contrast ratio	26.4	137.5	211.4	287.9
Dark state(8V)	3.79	0.73	0.47	0.35

The dark state of the RMM-OCB cell whose transmittance was decreased to 0.35% - 0.85% is much better than conventional OCB cell's. Without using OCB compensation films, the contrast ratio of the RMM-OCB cell can be up to about 287.9 from 26.4 which are measured from the conventional OCB cell. In other words, the contrast ratio of the RMM-OCB cell will be improved 11 times compared with conventional OCB cell.

Without using OCB compensation films, the contrast ratio of the RMM-OCB cell was enhanced from 26 of original OCB cell to about 288. In other words, the contrast ratio of the RMM-OCB cell was improved 11 times than conventional OCB cell.

We also use Conoscope to measure the RMM-OCB cell and the light source is white light. The results of dark state, bright state, and contrast state are shown in Fig. 4-J, Fig. 4-K, and Fig. 4-L.

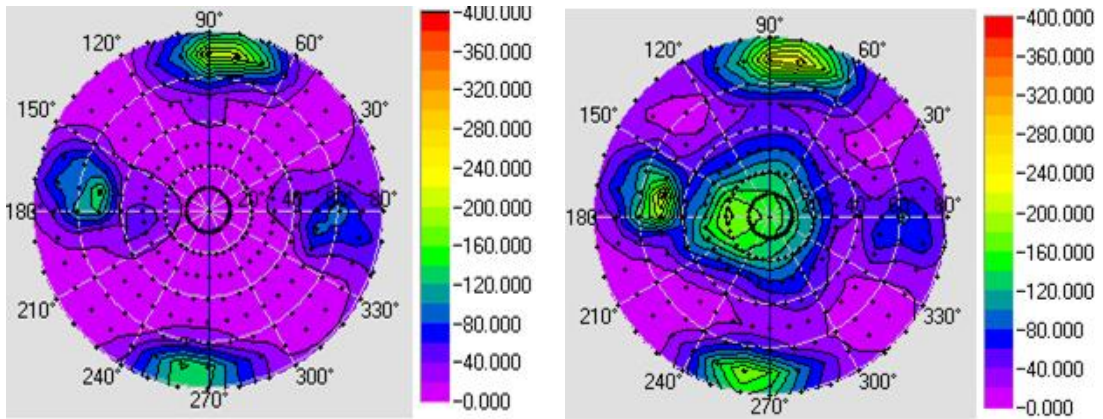


Fig.4-J (a) RMM-OCB cell under 7V (b) conventional OCB cell under 7V

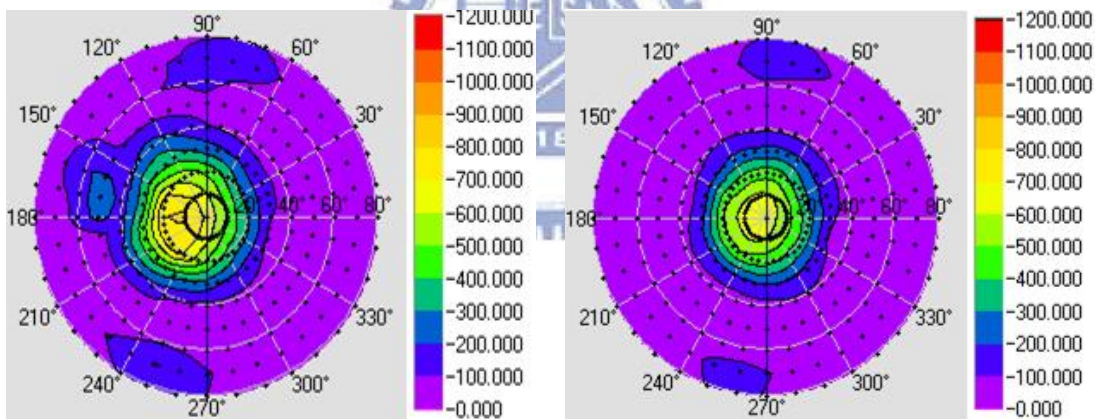


Fig.4-K (a) RMM-OCB cell under 0V (b) conventional OCB cell under 2V

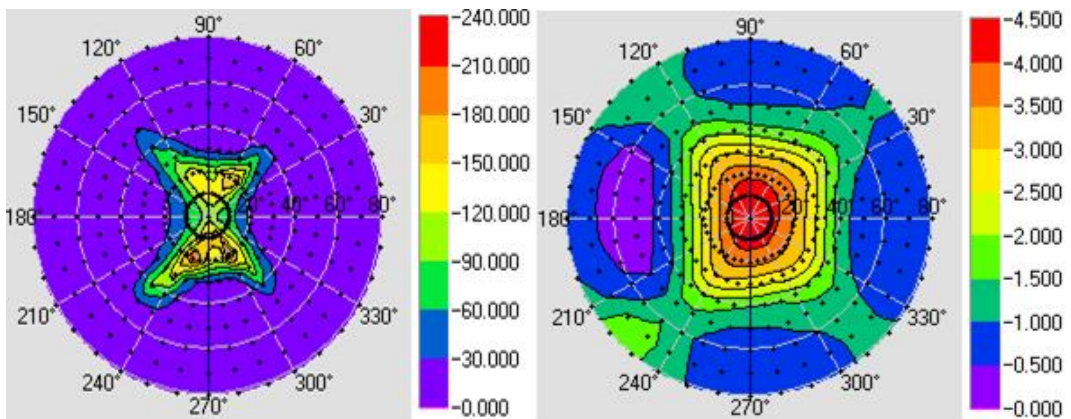


Fig.4-L (a) contrast state of RMM-OCB cell (b) contrast state of conventional OCB cell

From the figure, the dark state luminance of conventional OCB cell is $153.97(\text{cd}/\text{m}^2)$, but RMM-OCB cell only has $6.68(\text{cd}/\text{m}^2)$. It also proved the dark state of RMM-OCB cell is better than the conventional OCB cell, the light leakage is serious. In Figure 4-J (b), the bright state of RMM-OCB cell and conventional OCB cell are shown. The luminance of RMM-OCB cell is $690.11(\text{cd}/\text{m}^2)$, and for conventional OCB cell is $656.60(\text{cd}/\text{m}^2)$. From this point, the novel RMM-OCB cell didn't decrease the light intensity that passes through the cell. Furthermore, compare the dark state and bright state we can get the contrast ratio under white light. The contrast ratio for RMM-OCB cell is $\text{Cr}=103.27$ and for conventional OCB cell is $\text{Cr}=4.26$. As a result, the contrast ratio has been improved from 4 to 103, it is 24 times improved.

4-5 SUMMARIES



From the V-T measurement and the retardation measurement, the novel RMM-OCB cell can be proved phase transition free and stayed in a stable bend state initially. On the other hand, the RMM2-OCB cell became homeotropic and has no light transmittance under the V-T measurement. From the pretilt angle evaluation, the additional RMM layer can produce a pretilt angle higher than 75° . This could explain the phase transition free for the RMM-OCB cell and no transmittance for the RMM2-OCB cell. Moreover, the dark state of the RMM-OCB cell is darker than the conventional one from the V-T curves, and the result of Conoscope. The contrast ratio is improved up to 24 times under white light without using compensation films. With the advantages of high contrast ratio and no phase transition, the proposed RMM-OCB cell can achieve a good quality TFT-LCD and be more suitable for large size display applications in the near future.

CHAPTER 5

CONCLUSIONS

5-1 SUMMARY

In this research, no phase transition OCB cell can be achieved by an additional RMM layer on top of the PI layer, and that means no high pulse voltage for phase transition any more. Without phase transition, the R, G, B three colors won't be sacrificed because of the different critical voltage for different light wavelength. The RMM-OCB cell would stay in a stable bend state initially. No phase transition OCB cell possesses many other advantages, such as consume less power, and high transmittance at bright state. Moreover, the dark state of the RMM-OCB cell is darker than the conventional one from the T-V curves. The contrast ratio can be improved up to 11 times (from 26 to 288) without using compensation films. Besides, the RMM-OCB cell that we developed in this study requires no special drive circuit and compatible with the normal TFT drive method. Therefore, the proposed RMM-OCB cell can achieve a good quality TFT-LCD and be more suitable for large size display applications in the near future.

5-2 FUTURE WORKS

In this thesis, a novel structure was brought out to eliminate the phase transition of conventional OCB cell and the pretilt angle is higher than 75° . Because of the high pretilt angle, the RMM2-OCB cell became homeotropic and cannot have any light transmittance in the middle of polarizer and analyzer. When the concentration of RMM changed to a lower one and causes a thinner thickness of RMM layer, and change the PI material to a lower pretilt angle one, the RMM2-OCB cell might have some rooms to develop in the future.



REFERENCE

- [1] F. Reinizer, *Monatsh. Chem.*, **9**, 421 (1888)
- [2] O. Lehmann, *Z. Physik. Chem.*, **4**, 462 (1889)
- [3] P. J. Bos, J. A. Rahma, and J. W. Doane, *Society for Info. Disp. Symp. Digest Tech.*, **24**, 887 (1993)
- [4] Y. Tanaka, Y. Taniguchi, T. Sasaki, A. Takeda, Y. Koibe, and K. Okamoto, *Society for Info. Disp. Symp. Digest*, 206 (1999)
- [5] Y. Mishima, T. Nakayama, N. Suzuki, M. Ohta, S. Endoh, Y. Iwakabe, and H. Kagawa, *Society for Info. Disp. Symp. Digest*, 260 (2000)
- [6] J. W. Doane, D. K. Yang, and L. C. Chien, *International Disp. Research Conference Digest*, 175-178 (1991)
- [7] K. Iizuka, *Elements of Photonics, Volume I: In Free Space and Special Media*, (Wiley-Interscience, New York, 2002)
- [8] P. J. Bos, K.R. Koehler/Beran, *Mol. Cryst. Liq. Cryst.*, Vol. **113**, 329 (1984)
- [9] Y. Yamaguchi, T. Miyashita, T. Uchida, *SID*, San Jose, USA, February 1993, **19-04**, p. 277
- [10] P. J. Bos, P. A. Johnson, and K. R. Koehler-Beran, *Society for Info. Disp. Symp. Digest*, 30 (1983)
- [11] Y. Yamaguchi, T. Miyashita, and T. Uchida, *Society for Info. Disp. Symp. Digest*, 277 (1993)
- [12] C. L. Kuo, T. Miyashita, M. Suzuki, and T. Uchida, *Society for Info. Disp. Symp. Digest*, 927 (1994)

- [13]C. L. Kuo, T. Miyashita, M. Suzuki, and T. Uchida, *Jpn. J. Appl. Phys.*, part 2, **34**, L1362 (1995)
- [14]K. Kuboki, T. Miyashita, T. Ishinabe, and T. Uchida, *Mol. Cryst. Liq. Cryst.*, **410**, 391 (2004)
- [15]T. Miyashita, and T. Uchida, *IEICE TRANS. Electron*, NO.8 August, **E79-C**, 1076 (1996)
- [16]K. Kumagawa, A. Takimoto, and H. Wakemoto, *Society for Info. Disp. Symp. Digest*, 1288 (2002)
- [17]H. Mori and P. Bos, *Jpn. J. Appl. Phys.*, part 1, **38**, 2837 (1999)
- [18]H. G. Walton and M. J. Towler, *Liq. Cryst.*, **27**, 1329 (2000)
- [19]S. T. Wu and A. M. Lackner, *Appl. Phys. Lett.*, **64**, 2047 (1994)
- [20]J. E. Anderson, C. Chen, and A. Lien, U.S. Patent, No. 6,067,142 (23 May 2000)
- [21]K. Nakao, D. Suzuki, T. Kojima, M. Tsukane and H. Wakemoto, *Society for Info. Disp. Symp. Digest*, 1416 – 1419 (2004)
- [22]H. Kikuchi, H. Yamamoto, H. Sato, M. Kawakita, K. Takizawa and H. Fujikake, *Jpn. J. Appl. Phys.*, **44**, 981 (2005)
- [23]S. H. Kim and L. C. Chien, *Jpn. J. Appl. Phys.*, **43**, 7643 (2004)
- [24]N. Nagae, T. Miyashita and T. Uchida, *Society for Info. Disp. Symp. Digest*, 26 – 29 (2000)
- [25]E. J. Acosta, M. J. Towler and H. G. Walton, *Liq. Cryst.*, **27**, 977 (2000)
- [26]P. D. Brimicombe and E. P. Raynes, *Liq. Cryst.*, **32**, 1273 (2005)
- [27]P. D. Brimicombe and E. P. Raynes, *Appl. Phys. Lett.*, **89**, 031121 (2006)
- [28]D. W. Berreman, *J. Appl. Phys.*, **46**, 3746 (1975)
- [29]C. Z. Van Doorn, *J. Appl. Phys.*, **46**, 3738 (1975)
- [30]F. M. Leslie, *Arch. Ration., Mech. Anal.*, **28**, 265 (1968)
- [31]S. Onda, T. Miyashita and T. Uchida, *Asia Display*, 33-4 (1998)
- [32]S. H. Chen, and C. L. Yang, *Appl. Phys. Lett.*, **80**, 3721 (2002)

- [33] E. J. Acosta, M. J. Towler, and M. D. Tillin, *J. Appl. Phys.*, **97**, 093106 (2005)
- [34] N. Nagae, T. Miyashita, T. Uchida, Y. Yamada, and Y. Ishii, *Society for Info. Disp. Symp. Digest*, 26 (2000)
- [35] Y. Zhang, B. Wang, D. B. Chung, J. Colegrove and P. J. Bos, *SID*, Boston, USA, May 2005, **36**, 1782
- [36] J. Cheng, R. N. Thurston and D. W. Berreman, *J. Appl. Phys.*, **52**, p. 2756 (1981)
- [37] J. Cheng and R. N. Thurston, *J. Appl. Phys.*, **52**, p. 2766 (1981)
- [38] N. Koma, T. Miyashita, K. Yoneda and T. Uchida, *Society for Info. Disp. Symp. Digest*, **30**, 28 (1999)
- [39] X. D. Mi, M. Xu, D. K. Yang, and P. J. Bos, *Society for Info. Disp. Symp. Digest*, **30**, 24 (1999)
- [40] F. S. Yeung, Y. W. Li, and H. S. Kwok, *Appl. Phys. Lett.*, **88**, 041108 (2006)
- [41] T. Uchida, Y. Kimura, S. Kuniaki, H. Nakamura and Y. Taira, patent JP, 9 185 037 (1995)
- [42] C. Lee, H. Chang, J. Lyu, K. Kim and J. Souk, *Society for Info. Disp. Symp. Digest*, **33**, 570 (2002)
- [43] I. Inoue, T. Miyashita, T. Uchida, Y. Yamada, and Y. Ishii, Eurodisplay 2002, Nice, France, October, 179
- [44] E. Acosta, B. Henley, D. Kean, M. Tillin, C. Tombling, M. Towler, E. Walton, H. Walton, and R. Winlow, *Liq. Cryst.*, **31**, 1619 (2004)
- [45] C. G. Jhun, J. L. Lee, S. H. Kang, S. L. Lee, J. C. Kim, T. H. Yoon, J. D. Noh, D. H. Suh, and J. Y. Lee, *IDW'04*, 117 (2004)
- [46] K. Nakao, D. Suzuki, T. Kojima, M. Tsukane, and H. Wakemoto, *Society for Info. Disp. Symp. Digest*, 1416 (2004)
- [47] F. Bruyneel, H. D. Smet, J. Vanfleteren, and A. V. Calster, *Opt. Eng.*, **40**, 259 (2001)
- [48] S. H. Lee, T. Yoon, and J. C. Kim, *J. Appl. Phys.*, **100**, 064902 (2006)
- [49] Y. Sun, H. Ma, Z. Li, and Z. Zhan, *Appl. Phys. Lett.*, **90**, 091103 (2007)

[50]J. B. Kim, K. C. Kim, H. J. Ahn, B. H. Hwang, J. T. Kim, S. J. Jo, C. S. Kim, and H. K. Baika, *Appl. Phys. Lett.*, **91**, 023507 (2007)

[51]F. S. Yeung, Y. W. Li, and H. Kwok, *Appl. Phys. Lett.*, **88**, 041108 (2006)

